Science of the Total Environment 781 (2021) 146676

Contents lists available at ScienceDirect

Science of the Total Environment

journal homepage: www.elsevier.com/locate/scitotenv

Comparative sensitivity of the *early life stages* of a coral to heavy fuel oil and UV radiation

F. Mikaela Nordborg [a,b,c,*], Diane L. Brinkman [c], Gerard F. Ricardo [c], Susana Agustí [d], Andrew P. Negri [a,c]

[a] AIMS@JCU, Division of Research & Innovation, James Cook University and Australian Institute of Marine Science, Townsville 4810, Queensland, Australia
[b] College of Science & Engineering, Division of Tropical Environments and Societies, James Cook University, Townsville 4810, Queensland, Australia
[c] Australian Institute of Marine Science, Townsville 4810, Queensland, Australia
[d] Red Sea Research Centre, King Abdullah University of Science and Technology, Biological Environmental Science and Engineering Division, Thuwal 23955, Saudi Arabia

HIGHLIGHTS

- Oil pollution from shipping remains a significant threat in coral reef environments.
- The effects of heavy fuel oil and UVR on early coral life stages were assessed.
- Heavy fuel oil negatively affects all early life stages of *Acropora millepora*.
- Assessed endpoints among the most sensitive for aquatic organisms tested to date
- UVR significantly increases heavy fuel oil toxicity to early life stages of coral.

GRAPHICAL ABSTRACT

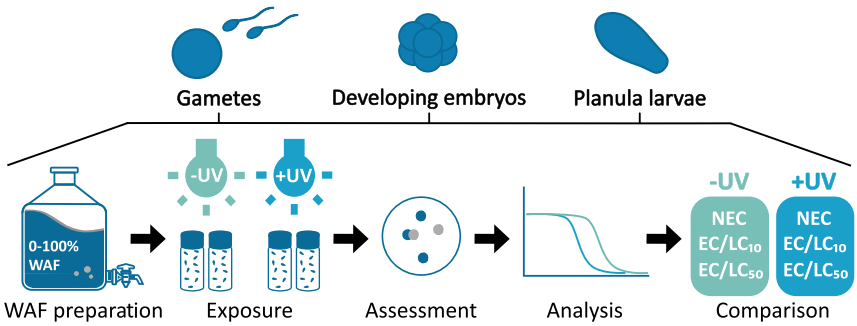

ARTICLE INFO

Article history:
Received 26 January 2021
Received in revised form 17 March 2021
Accepted 18 March 2021
Available online 23 March 2021

Editor: Thomas Kevin V

Keywords:
Petroleum oil
PAH
Pollution
Ultraviolet radiation
Phototoxicity
Coral reefs

ABSTRACT

During an oil spill, shallow, tropical coral reefs are likely to be simultaneously exposed to high intensities of ultraviolet radiation (UVR), which can exacerbate the toxicity of petroleum oils. While successful recruitment of corals is critical for reef recovery following disturbances, the sensitivity of several early life stages of coral to petroleum hydrocarbons has not been investigated, particularly for UVR co-exposure. Here we present the first dataset on the relative sensitivity of three early life stages (gametes, embryos and planula larvae) in a model broadcast spawning coral species, *Acropora millepora*, to the dissolved fraction of a heavy fuel oil (HFO), both in the absence and presence of UVR. All early life stages were negatively impacted by HFO exposure but exhibited distinct sensitivities. Larval metamorphosis was the most sensitive endpoint assessed with a 10% effect concentration of 34 μg L^{-1} total aromatic hydrocarbons (TAH) in the absence of UVR. The impact on fertilisation success was highly dependent on sperm density, while the fragmentation of embryos masked embryo mortality. Larval metamorphosis was conclusively the most reliable endpoint for use in risk assessments of the endpoints investigated. Putative critical target lipid body burdens (CTLBBs) were calculated for each life stages, enabling a comparison of their sensitivities against species in the Target Lipid Model (TLM) database. *A. millepora* had a putative CTLBB of 4.4 μmol g^{-1} octanol for larval metamorphosis, indicating it is more sensitive than any species currently included in the TLM database. Coexposure to UVR reduced toxicity thresholds by 1.3-fold on average across the investigated life stages and endpoints. This increase in sensitivity in the presence of UVR highlights the need to incorporate UVR co-exposure (where ecologically relevant) when assessing oil toxicity thresholds, otherwise the risks posed by oil spills to shallow coral reefs are likely to be underestimated.

© 2021 The Author(s). Published by Elsevier B.V. This is an open access article under the CC BY-NC-ND license (http://creativecommons.org/licenses/by-nc-nd/4.0/).

* Corresponding author at: AIMS@JCU, Division of Research & Innovation, James Cook University and Australian Institute of Marine Science, Townsville 4810, Queensland, Australia.
E-mail address: mikaela.nordborg@my.jcu.edu.au (F.M. Nordborg).

https://doi.org/10.1016/j.scitotenv.2021.146676
0048-9697/© 2021 The Author(s). Published by Elsevier B.V. This is an open access article under the CC BY-NC-ND license (http://creativecommons.org/licenses/by-nc-nd/4.0/).

1. Introduction

Oil pollution is a substantial local threat to coral reefs with large-scale spills posing a potential risk anywhere commercial shipping, oil extraction or oil processing occurs. While large scale spill events are rare, the consequences in reef environments can be catastrophic (Jackson et al., 1989; Guzman et al., 2020) and spill incidents continue to occur in tropical and subtropical seas (Diercks et al., 2010; Storrie, 2011; Sun et al., 2018; The Guardian, 2018; Daley, 2019; Asariotis and Premti, 2020). Coral reefs are facing increasing global threats from warming and acidification of the ocean (Hoegh-Guldberg et al., 2017; Hughes et al., 2018) and reducing local pressures such as pollution is a key management strategy to maximise coral reef resilience as the climate changes (Hughes et al., 2017; MacNeil et al., 2019). The effective management of oil pollution hazards in tropical ecosystems requires an understanding of their potential impacts on reef-building corals (Turner and Renegar, 2017; Nordborg et al., 2020), as the condition of these habitat-forming taxa will have widespread consequences on the ecosystem as a whole (Sorokin, 2013).

Oil pollution is unlikely to be the only stressor faced by a coral reef during a spill event. Other environmental pressures, including temperature, light availability, ultraviolet radiation (UVR), ocean acidification, salinity, nutrients and sediments, can affect the health of corals with several environmental factors commonly affecting reef health simultaneously (Ban et al., 2014; Ellis et al., 2019). Co-exposure to UVR is almost certain during oil spills affecting shallow-water coral reefs, which are mainly found in oligotrophic, tropical (0–30° latitude) waters where UVR exposure is high throughout the year (Nordborg et al., 2020). UVR directly affects coral health and interacts with other environmental factors, including increasing coral bleaching during marine heatwave events (Banaszak and Lesser, 2009). Dissolved polycyclic aromatic hydrocarbons (PAHs) are the primary cause of acute toxic effects observed for pelagic and benthic organisms during spill events (Di Toro et al., 2000; French-McCay, 2002) and UVR increases the toxicity of many PAHs, generally referred to as phototoxicity (Pelletier et al., 1997; Barron, 2017). PAH phototoxicity can occur through two main pathways: photosensitisation or photomodification/photooxidation with the pathway dependent on the molecular structure of the PAH and when UVR exposure occurs (prior to or following uptake of PAHs by an organism) (Barron, 2017). However, a combination of both mechanisms is likely to contribute to the total toxicity observed during a spill on or near tropical coral reefs (Nordborg et al., 2020).

The success of the early life stages of coral is critical for recruitment and recovery of coral reefs following disturbances (Harrison and Wallace, 1990). Yet, only limited information is available that describes which coral life stages may be sensitive to combined oil and UVR exposures (Nordborg et al., 2020). The majority of scleractinian coral species are broadcast spawners, which release gametes into the water column for fertilisation and development (Harrison and Wallace, 1990; Baird et al., 2009). Following gamete release, the lipid rich eggs and embryos of most species will ascend towards the surface and remain there during embryonic and early larval development. The time from fertilisation until larvae reach settlement competency (ability to attach and metamorphose into a sessile primary polyp) varies from 24 h to over one week across described species (Jones et al., 2015; Randall et al., 2020). This time interval spent at, or close to, the surface represents a high-risk period of simultaneous exposure to dissolved PAHs from an oil spill and high UVR intensities during the day. Most studies investigating oil toxicity thresholds for reef-building corals have not included UVR as a co-factor (Turner and Renegar, 2017; Nordborg et al., 2020), and when UVR is considered the exposure methodology varies widely (Nordborg et al., 2020). While laboratory studies have tested the phototoxicity of oils and individual aromatics towards adult coral colonies (Peachey and Crosby, 1995; Guzmán Martínez et al., 2007) and larvae (Peachey and Crosby, 1995; Negri et al., 2016; Nordborg et al., 2018; Overmans et al., 2018), it remains unclear which coral life stages are most sensitive to oil exposure, in either the presence or absence of UVR (Nordborg et al., 2020). Despite more than four decades of oil toxicity research on corals (Birkeland et al., 1976; Rinkevich and Loya, 1979), no comparative studies of the relative sensitivity between multiple life stages have been published (Turner and Renegar, 2017; Nordborg et al., 2020). Furthermore, the sensitivity of several early life stages of coral, including developing embryos, newly settled recruits and juvenile corals, have not been reported (Turner and Renegar, 2017; Nordborg et al., 2020), preventing their consideration in risk assessments.

To address these issues, the present study aims to: (i) identify the early life stage(s) that are most sensitive to oil exposure in a model coral species; (ii) quantify the impact of UVR co-exposure on toxicity for each life stage assessed; (iii) identify toxicity threshold concentrations applicable in risk assessments for tropical coral reef environments; and (iv) identify ecologically relevant, sub-lethal endpoints that are suitable for use in future coral oil toxicity research. These objectives were achieved by exposing three distinct early life stages of *Acropora millepora* to the water accommodated fractions (WAFs) of a heavy fuel oil (HFO) in the presence and absence of artificial UVR with intensity and spectral qualities representative of conditions occurring on mid-shelf reefs on the central Great Barrier Reef (GBR; Queensland, Australia) (Nordborg et al., 2018).

2. Methods

2.1. Coral collection

Gravid *A. millepora* colonies for all but one assay (the preliminary gamete assay) were collected from nearshore or mid-shelf reefs on the central GBR under Great Barrier Reef Marine Park Authority permits G12/35236.1 and G19.43024. Colonies were collected in the days leading up to the respective October, November or December full moon and transported in shaded plastic flow-through aquaria to the National Sea Simulator at the Australian Institute of Marine Science. On arrival colonies were transferred to flow-through holding tanks and maintained in 1 μm filtered natural seawater (FSW) at 27 °C under 70% shaded natural sunlight until spawning occurred. Refer to Tables S1 and S8 in Supplementary materials for details of parent origin for individual assays.

2.2. Preparation and chemical analysis of treatment solutions

HFO (International Bunker Supplies Pty Ltd, Gladstone, Australia), received as two separate batches (Sep 2016 and Feb 2018), was used to prepare WAFs for each assay as previously described (Negri et al., 2016; Nordborg et al., 2018) in accordance with standardised procedures for the preparation of low energy WAFs (Singer et al., 2000; Barron and Ka'aihue, 2003; Aurand and Coelho, 2005). Briefly, HFO was applied to the surface of 0.5 μm FSW in a solvent-rinsed glass aspirator at a loading of 20 g oil L^{-1}. The mixture was stirred without forming a vortex (180 rpm) for 16–26 h at room temperature (21 ± 1 °C), protected from light. The mixture was allowed to settle for ~30 min and 100% WAF was gently drained via a tap at the bottom of the aspirator. The 100% WAF was diluted using FSW to seven or more treatment concentrations for each assay performed (Barron and Ka'aihue, 2003; Forth et al., 2017). Treatment solutions were used within 24 h unless otherwise specified (Aurand and Coelho, 2005). See also Table S2 for specific details on WAF preparation for each experimental assay.

WAF samples for chemical analysis were collected for each assay at the start and end of exposures (Barron and Ka'aihue, 2003). Undiluted WAF was collected directly from the aspirator bottle at the start of each experiment. Glass scintillation vials containing undiluted WAF (n = 30) were exposed to the same conditions as the test organisms in the +UVR and −UVR incubators (Nordborg et al., 2018), and pooled WAF was sampled post-exposure. Samples were collected in solvent rinsed, 40 mL volatile organic compound (VOC) vials with

polytetrafluoroethylene (PTFE) septa and 500 mL amber glass bottles with PTFE-lined caps, acidified to pH 2 using 6 M hydrochloric acid and stored at 4 °C. Neat 2018 HFO and WAF samples were shipped to ChemCentre (Perth, Australia) for GC–MS analysis of benzene, toluene, ethylbenzene and xylenes (BTEX; USEPA method 8260), PAHs, including alkyl-substituted PAH (USEPA method 8270), and GC-FID analysis of total recoverable hydrocarbons (TRH; NEPM (2013)) as described previously (Negri et al., 2016; Nordborg et al., 2018). Neat 2016 HFO characterisation was reported in Nordborg et al. (2018). The time-weighted average concentrations of measured total aromatic hydrocarbons (TAH; $\sum$(BTEX and PAH)) in pre- and post-exposure WAFs, expressed as μg L^{-1}, were used for statistical analyses, toxicity modelling and derivation of putative CTLBBs.

2.3. Experimental assays

Three separate experimental assays were performed, each targeting a discrete early life stage or life stage transition of *A. millepora*. Exposure time was individually determined for each life stage to meet the criteria for chronic exposure as defined by the Australian and New Zealand Water Quality Guideline-framework (Warne et al., 2018). For details on treatment concentrations, water quality parameters, incubation temperature, and light conditions for individual assays, refer to Tables S2–S3.

To assess the impact of the available light spectrum on HFO WAF toxicity, assays for gamete, embryo and larval stages were performed under various light treatments: visible light and UVR (+UVR), visible light without UVR (−UVR), or in darkness (Dark) (see Tables 1 and S3 for treatment combinations and light conditions used in individual assays). Glass vials containing treatment solutions and corals were randomly placed within orbital shaker incubators (Thermoline Scientific, Australia), either upside down (gametes) or on their sides (embryos and planula larvae). Both −UVR and +UVR incubators were fitted with photosynthetically active LED lights (Aqualina Blue 450 nm, 10,000 K and 420 nm Actinic LED strips, Aqualina Lighting Australia) and vials were exposed under a 12:12 h constant light:dark cycle (~50–80 μmol quanta m^{-2} s^{-1}). In addition to visible light, vials in the +UVR treatments were exposed to UVR on a 6:18 h light:dark UVR cycle (~1.3–1.6 mW cm^{-2}; ~98% UVA and ~2% UVB) using UVR emitting fluorescent tubes (T8; 18 W Deluxlite BLB and 18 W ReptileOne UVB 5.0). See Table S3 for specific details of light treatments used for individual assays and refer to Nordborg et al. (2018) for spectral profile of UVR fluorescent tubes.

2.4. Fertilisation assay

A. millepora eggs (1 genotype) and sperm (4 or 8 genotypes) were collected, separated and cleaned as per Negri et al. (2011) on spawning nights in 2018 and 2019 from gravid colonies. Sperm were pooled and, depending on the resultant sperm density (determined using a hemocytometer, n = 6 counts), diluted using 0.5 μm FSW. Aliquots (0.5 mL) of egg (~100 eggs) or sperm solution were pipetted into replicate vials containing 8.5 mL of treatment solution (n = 6 per treatment combination and gamete type; n = 12 for FSW controls). Gametes were pre-exposed to ≥8 treatment concentrations (0–766.4 μg L^{-1} TAH) for 30 min under each light treatment (Dark, −UVR and +UVR), and fertilisation was initiated by gently transferring the sperm-WAF solutions into the corresponding egg vials. The primary assay was conducted at an optimal final sperm density of 1.2×10^6 sperm mL^{-1} (Ricardo et al., 2015). Additionally, a sub-optimal sperm density was used (1.5×10^3 sperm mL^{-1}) to assess if thresholds are sperm-density dependant (dark only; Ricardo et al. (2018)). Exposure continued under each respective light treatment for ~3 h post fertilisation (hpf) at 27 °C (0 rpm; Orbital shaker incubator, Thermoline Scientific, Australia), and was terminated when 4-cell embryos were observed in reference FSW samples. Samples were fixed by adding ~4 mL of fixative (10% formaldehyde and 5% Na-β-glycerophosphate in FSW) to the bottom of each replicate vial followed by gentle swirling. Fertilisation success was assessed directly in sealed sample vials by manual counting of unfertilised eggs and cleaved embryos under a dissecting microscope.

2.5. Embryonic and larval development assay

A. millepora embryos at *prawn chip/bowl*-stage (~12 hpf) exhibiting normal morphology were collected from a single mass culture (prepared as per Nordborg et al. (2018)) and gently washed in clean 0.5 μm FSW. Embryos (~600–800 μm diameter) were gently transferred to glass scintillation vials (10 per vial) in <1 mL of FSW using wide mouthed, disposable Pasteur pipettes. Treatment solution (20 mL; ~10% headspace) was added to each replicate vial (n = 6 per treatment combination, n = 12 for FSW controls) and embryos were exposed to 10 treatment concentrations (0–849.8 μg L^{-1} TAH) for 48 h under visible light in the presence (+UVR) or absence (−UVR) of UVR at 27 °C. Gentle shaking (~70 rpm; Orbital shaker incubator, Thermoline Scientific, Australia) commenced after ~24 h of exposure when embryos had reached the *gastrula* stage. Vial locations within each incubator were randomized once per 24 h, and survivorship assessed after 48 h, during which surviving embryos had completed development into planula larvae. Living larvae (defined as pigmented and/or swimming) were transferred to fresh 0.5 μm FSW in 6-well plates to recover in the absence of UVR and dissolved aromatics until 9 days post-fertilisation. FSW changes were performed every 48 h and survival re-assessed at 2-, 6- and 7-days post-exposure. Additionally, qualitative notes on larval morphology and behaviour (activity level, position within vials or wells, and abnormalities) were recorded during each assessment.

2.6. Larval survival and metamorphosis assay

A. millepora planula larvae (6- or 7-day old) collected from a single larval culture were exposed to 10 concentrations of HFO WAF (0–985 μg L^{-1} TAH) as per Nordborg et al. (2018). Briefly, larvae were transferred to glass scintillation vials (n = 6 vials per treatment combination, n = 12 vials for FSW controls) and 20 mL of treatment solution was gently added (~10% headspace). Vials were capped tightly and placed randomly in the +UVR or −UVR orbital shaker incubators (27 °C, 70 rpm) and exposed for 48 h. Vial locations within incubators were randomized once per 24 h. At 48 h, larvae were transferred to 6-well plates in 10 mL of treatment solution, survival assessed, treatment information replaced with an ID code, and settlement induced using 5 or 10 μL crustose coralline algae extract (prepared from *Porolithon onkodes*; Heyward and Negri (1999); Negri et al. (2005)). After ~24 h incubation at 27 °C (12:12 h L:D of visible light −UVR), metamorphosis success was assessed blind using a dissecting microscope. Notes were taken regarding larval and recruit morphology, abnormalities, fragmentation, recruit metamorphosis state and the general state of samples (e.g. degradation, presence of lipids, etc.). When present, the number of larval fragments, underdeveloped recruits and abnormal/deformed larvae or recruits was recorded.

Larvae were considered to have undergone metamorphosis if they had changed from planula larva to primary polyp. This included larvae that had formed disc-shaped structures with flattening of the oral-aboral axis and visible septal mesenteries radiating from the central mouth region (Heyward and Negri, 1999), most of which had attached firmly to the well plates. Larvae that had undergone early stage metamorphosis with permanent attachment and flattening but incomplete development of the central mouth region were also included, as these may be capable of continuing to full development after the 24 h incubation period.

2.7. Statistical analysis

Proportional decline in the response for each endpoint was modelled as a function of log concentration of HFO WAF using Bayesian non-linear models through the jagsNEC package (Fisher et al., 2020) in the software R (version 4.0.2; R Core Team (2020)) and the RStudio interface (RStudio Team, 2020). No effect concentrations (NEC; Pires et al. (2002); Fox (2010)), as well as 10% and 50% lethal or effect concentrations (LC/EC_{10} and LC/EC_{50}), were derived from the median of the model averaged concentration-response curves, using the inbuilt package functions as appropriate, and presented with 95% credible intervals. The model-averaging approach uses weighted-average predictions based on deviance information criterions (DIC) for each candidate model as described by Fisher et al. (2020). Candidate models included commonly used concentration-response relationship models as well as functional NEC threshold models adapted from Fox (2010). All candidate models were initially fit using the binomial distribution. If strong evidence of overdispersion was observed for individual candidate models they were excluded from the final model subset. If all candidate models showed strong evidence of overdispersion, models were re-fitted using a beta distribution unless otherwise indicated. The specific priors, burn-in length and iterations (minimum 20,000) used for each dataset was selected based on data type and model diagnostics (convergence, chain mixing, evidence of autocorrelation, overdispersion and visual inspection of model fit). Where multiple light treatments were tested, differences in threshold values (i.e. NEC, LC/EC_{10} or LC/EC_{50}) between light treatments were analysed using the inbuilt functions of the jagsNEC package, which follow Labelle et al. (2019). Briefly, the difference between the posteriors for each modelled toxicity threshold concentration was calculated, and the probability (in %) that one light treatment had a larger threshold value than the other was estimated. Additionally, the posterior, median and 95% credible intervals of the threshold values for each comparison were presented graphically. See also Table S4 for full details on distributions and candidate models used for individual datasets and assays. If no, or insufficient, concentration-response was observed for one of the applied light treatments in an experimental assay (based on statistical analysis), no comparisons of NEC or EC/LC_{50} posteriors were performed. For details on the data quality assessment and exclusion of individual replicates from statistical analysis for each life stage assessed refer to Section S4. Statistical analysis, Supplementary materials.

2.8. Calculation of putative CTLBBs

The most effective method to compare the sensitivity of species or endpoints to aromatic hydrocarbon exposure is to derive species-specific CTLBBs (also referred to as critical body residues; CBR), which are independent of both WAF and neat oil composition (Di Toro et al., 2000; French-McCay, 2002; Redman and Parkerton, 2015). Species-specific CTLBBs for a defined endpoint are derived using the TLM, which is based on the linear relationship between log EC/LC_{50} and log K_{OW} (octanol-water partitioning coefficient) for non-polar narcotic chemicals, including aromatic hydrocarbons (Di Toro et al., 2000; French-McCay, 2002; McGrath and Di Toro, 2009). Experimental toxicity data for at least three aromatic hydrocarbons of varying K_{OW} are required to derive a definitive CTLBB estimate from the y-intercept of the regression. The CTLBB can then be used to predict the narcotic toxicity of any dissolved aromatic hydrocarbon in terms of EC/LC_{50} or *toxicity units* (TUs), where its dissolved concentration is normalised by its predicted toxicity (Di Toro et al., 2000; French-McCay, 2002; Redman et al., 2012). In complex hydrocarbon mixtures, the contribution of individual hydrocarbon TUs to overall toxicity is additive (Di Toro et al., 2007).

As no single aromatic toxicity data are currently available for *A. millepora*, putative CTLBBs were modelled from the experimental EC/LC_{50} values for each endpoint and the time-averaged concentrations of individual aromatic hydrocarbons measured in the associated WAF. The TLM was initially parameterised as per McGrath et al. (2018), using a universal slope of -0.940 mmol L^{-1}, the geomean CTLBB value of 71.1 μmol g^{-1} octanol for 79 species in the TLM database, and chemical class corrections for BTEX (-0.025) and PAHs (-0.346) to account for their higher potency compared to baseline narcotic chemicals. Physico-chemical data were sourced from EPI Suite 4.11 (USEPA, 2012). Individual aromatic hydrocarbon TUs were calculated by dividing each measured concentration by the corresponding TLM-predicted EC/LC_{50} value and the TUs were summed to obtain TU_{mix}. The Excel Goal Seek algorithm was then used to solve for the CTLBB that produced a modelled EC/LC_{50} ($TU_{mix} = 1$) equal to the experimentally derived EC/LC_{50} value.

3. Results

3.1. Chemical analysis

The HFO used to produce WAFs was supplied in two separate batches (2016 and 2018). The embryo and larval assays were performed using the 2016 batch and the 2018 batch was used for the fertilisation assays. The neat oils contained a similar suite of aromatics (Table S5), but the concentration of PAHs in the 2016 HFO (50,494 mg kg^{-1}) was approximately twice that of the 2018 HFO (24,150 mg kg^{-1}), primarily due to the 1.9- to 3.0-fold higher concentrations of naphthalene and C1- to C4-alkylnaphthalenes (Table S5). The time-averaged concentrations in the corresponding undiluted WAFs also differed, with the 2016 HFO WAFs containing a higher average TAH concentration than the 2018 HFO WAFs (839 μg L^{-1} ($n = 6$) and 426 μg L^{-1} ($n = 3$), respectively; Table S6) and a higher proportion of PAHs (70% of TAH compared to 57%, respectively). This difference is mainly attributed to the 3.6- and 1.8-fold higher concentrations of naphthalene and C1-alkylnapthalenes, respectively (Table S6). However, across all WAFs, BTEX and the naphthalene series collectively constituted 97–98% of time-weighted TAH concentrations (Table S6). For complete chemical analysis results of WAFs and neat oils refer to Tables S5–S7 and Figs. S1–S2.

3.2. Fertilisation assay

Fertilisation success of *A. millepora* gametes was dependent on sperm density, dissolved TAH concentration and the light treatment applied during HFO exposure. Higher TAH concentrations resulted in decreased fertilisation success in all light treatments (Fig. 1a), and inhibition of fertilisation in the dark occurred at lower TAH concentrations (21.0 μg L^{-1} TAH; NEC) under sperm-limited conditions compared to optimal-sperm conditions (292 μg L^{-1} TAH; NEC) (Fig. 1a, Table 1). However, the magnitude of inhibition was highly dependent on light treatment, with UVR co-exposure decreasing EC_{50}s by greater than 70-fold compared to visible light and dark treatments at optimal-sperm conditions: 5.3, 375 and >432 μg L^{-1} TAH, respectively (Fig. 1b, Table 1).

NEC and 10% effect concentrations followed similar trends with inhibition of fertilisation occurring at very low concentrations (3.7 and 3.5 μg L^{-1} TAH, respectively) in the presence of UVR (Table 1). Fertilisation success in FSW controls was strongly dependent on sperm density, averaging 82% at optimal sperm densities ($1.2 \cdot 10^6$ sperm mL^{-1}) and 25% under sperm-limited conditions ($1.5 \cdot 10^3$ sperm mL^{-1}) in the absence of light (Fig. 1a).

3.3. Embryonic and larval development assay

Survival during embryonic development in *A. millepora* was affected by TAH concentration, light treatment and time since fertilisation, with latent effects increasing after the 48 h exposure. At the end of exposure, surviving embryos had completed development into planula larvae, and average survival in controls at 48, 96 and 192 h was 112%, 101% and 96%, respectively (Fig. 2a, c and e). The apparent increase in survival at the

Table 1
Interpolated threshold concentrations for each assay performed and putative CTLBBs. The relative sensitivity of each of the life stages tested is also provided based on a fitted lognormal SSDs of the 79 species CTLBBs in the TLM database (McGrath et al., 2018). NEC and EC/LC_x given as median of the posterior distribution in μg TAH L^{-1} with 95% credible intervals (in brackets). For details of which model subsets were included in the final models, and the distributions used, refer to Table S4 and R scripts.

Life stage	Endpoint	Light regime	NEC (μg TAH L^{-1})	EC/LC_{10} (μg TAH L^{-1})	EC/LC_{50} (μg TAH L^{-1})	$CTLBB_{EC/LC50}$ (μmol g^{-1} octanol)	Sensitivity rel. to spp. in TLM (%)
Gametes	Fertilisation[a] ($1.5 \cdot 10^3$ sperm mL^{-1})	Dark	21.0 (8.8–89.2)	30.4 (10.1–99.0)	141 (74.0–341)	8.3 (4.4–20.1)	0.53 (0.05–6.7)
	Fertilisation ($1.2 \cdot 10^6$ sperm mL^{-1})	Dark	292 (209–333)	329 (273–360)	>432	–	–
		−UVR	198 (101–289)	174 (114–236)	375 (342–417)	15.1 (13.8–16.8)	3.3 (2.6–4.3)
		+UVR	3.7 (4.1–4.3)	3.5 (1.6–4.3)	5.3 (4.4–8.6)	–	–
Embryos	48 h survival	−UVR	>843	>843	>843	–	–
		+UVR	192 (70–304)	354 (240–540)	>850	–	–
	96 h latent survival	−UVR	103 (78.2–140)	111 (70.9–186)	164 (126–208)	9.6 (7.3–12.1)	0.86 (0.34–1.8)
		+UVR	270 (134–406)	268 (170–402)	296 (216–405)	–	–
	192 h latent survival	−UVR	128 (95.1–172)	131 (98.6–173)	157 (126–195)	9.2 (7.3–11.4)	0.75 (0.34–1.5)
		+UVR	272 (163–406)	267 (0–410)	290 (217–413)	–	–
Planula larvae	Survival	−UVR	373 (356–379)	375 (306–380)	399 (382–481)	21.6 (20.6–26.0)	7.8 (7.0–12)
		+UVR	166 (139–183)	161 (122–194)	328 (267–391)	–	–
	Fragmentation	−UVR	184 (171–189)	186 (175–190)	196 (191–209)	10.6 (10.3–11.3)	1.2 (1.1–1.4)
		+UVR	132 (99–189)	128 (0–186)	139 (102–192)	–	–
	Metamorphosis	−UVR	88.3 (75.7–96.9)	33.8 (22.3–48.2)	81.4 (70.9–94.5)	4.4 (3.8–5.1)	0.05 (0.03–0.09)
		+UVR	41.3 (34.3–44.8)	21.2 (14.4–29.8)	63.8 (54.7–74.1)	–	–

– = CTLBB not derived.
[a] TRH and BTEX concentrations were estimated, refer to Table S6.

end of the 48 h exposure in some replicates (controls and treatments) resulted from fragmentation of embryos during exposure and subsequent development of the fragments into smaller than normal larvae (i.e. <1 mm length). After transfer to clean FSW the average survival (including normal sized larvae and smaller larvae resulting from embryonic fragmentation) relative to the start of exposure remained high (>80%) for seawater controls, as well as low-mid concentrations (<100 μg L^{-1} TAH) at the 96 and 192 h assessments (Fig. 2c and e).

At the end of the 48 h HFO WAF exposure, impacts on embryonic survival were only observed at high TAH concentrations (>192 μg L^{-1} TAH) in the presence of UVR (Fig. 2a, Table 1). No LC_{50} could be derived at 48 h but the derived NEC and LC_{10} were reduced by at least 4.4- and 2.4-fold in the presence of UVR, respectively, indicating phototoxicity (Fig. 2b, Table 1). While limited impacts were observed at 48 h, latent survival (after transfer to FSW) was significantly affected at substantially lower TAH concentrations for both light treatments. The latent impacts observed on survival were similar at 96 and 192 h (Fig. 2c and e, Table 1), with LC_{50} estimates at both time points decreasing by at least 2.9- and 5.1-fold in the presence and absence of UVR, respectively, compared to corresponding values at the end of 48 h exposure (Table 1). In contrast to 48 h survival profiles, the latent impacts after 96 and 192 h were greater for larvae exposed to HFO in the absence of UVR, with all threshold values 1.8- to 2.6-fold lower than corresponding estimates in the presence of UVR, respectively (Fig. 2d and f, Table 1).

3.4. Larval survival and metamorphosis assays

Larval survival and metamorphosis success in *A. millepora* were affected by the TAH concentration and light treatment applied during

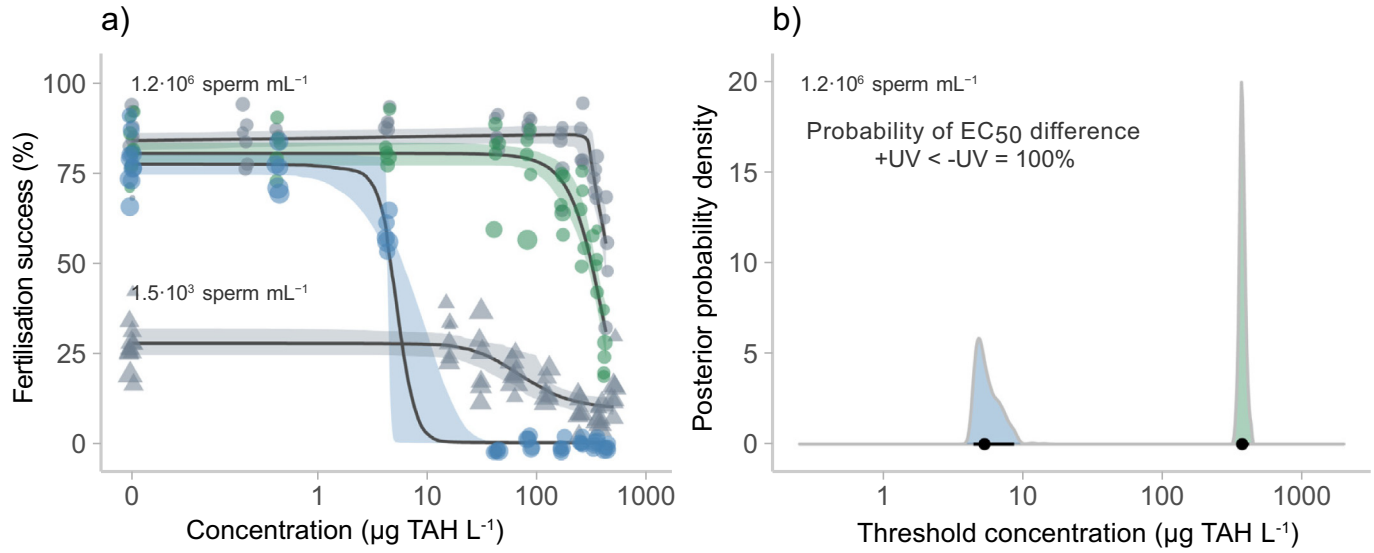

Fig. 1. Fertilisation success of *A. millepora* gametes exposed to HFO WAFs under three different light regimes at two sperm densities (a) and the PPDD for fertilisation success EC50s (b). Gametes exposed to HFO WAF in the absence of light (grey; Dark), under visible light in the absence of UVR (green; −UVR) or under visible light in the presence of UVR (blue; +UVR). For a) the model median (solid line), 95% credible intervals (shaded band) and raw data points are shown for assays performed in 2018 (triangles) and 2019 (circles). Sperm density used in assays indicated above corresponding model median lines. Size of raw data points is indicative of the total number of eggs and embryos assessed for individual replicates. For b) PPDD median (solid dot) and 95% credible intervals (solid line) shown for +UVR and −UVR treatments. For corresponding graphical representations of the NEC model subset refer to Fig. S3. For interpretation of the references to colour in this figure legend, the reader is referred to the web version of this article.

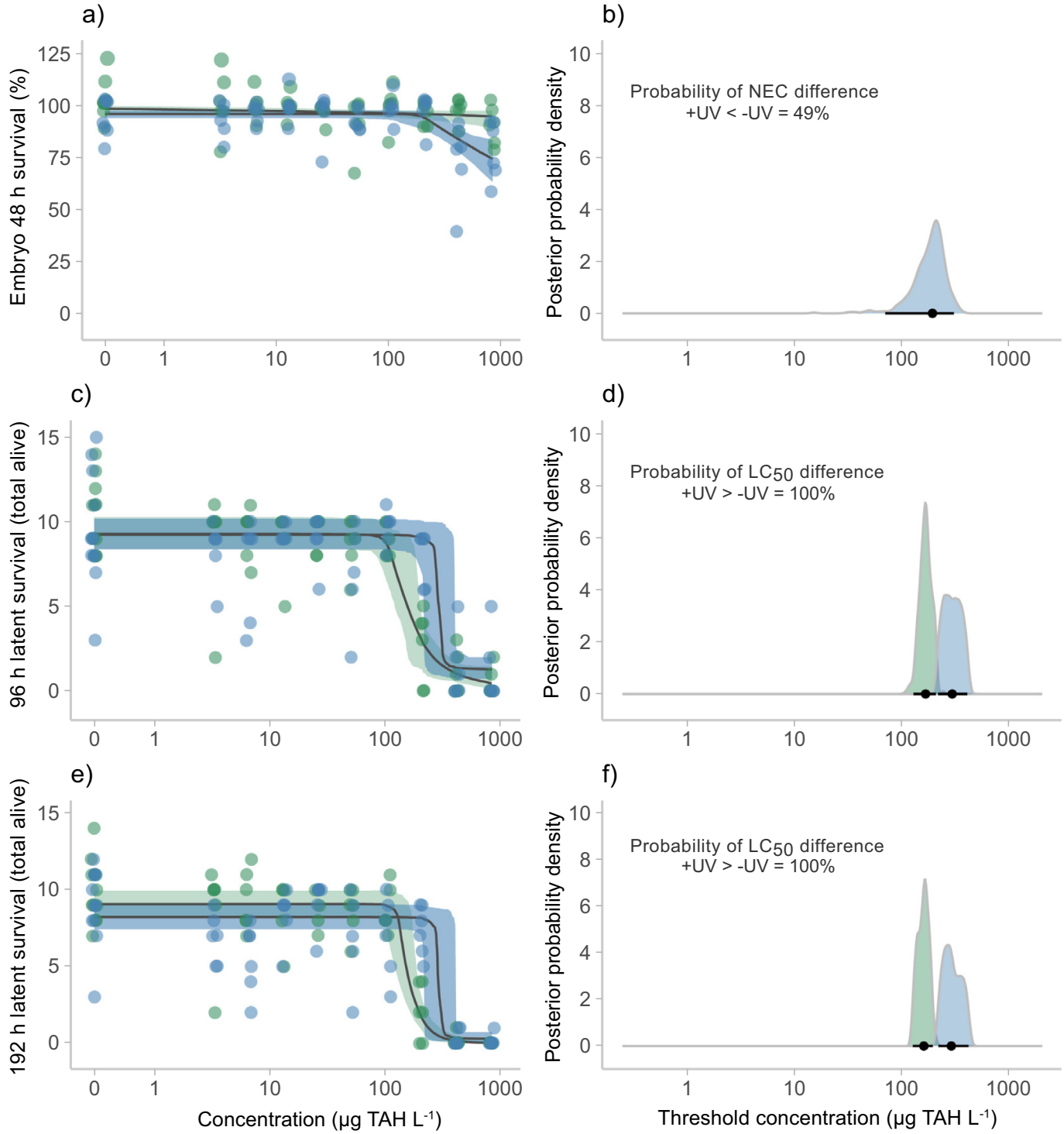

Fig. 2. Direct (a) and latent (c and e) survival of *A. millepora* embryos exposed to HFO WAFs, under visible light in the absence (green; −UVR) or presence (blue; +UVR) of UVR, and the PPDD for threshold concentrations derived for each time point (b, d and f). Model median (solid line), 95% credible intervals (shaded band) and raw data points (circles) are shown for each assessment. PPDD median (solid dot) and 95% credible intervals (solid line) shown for each endpoint. Please note that the comparison of threshold concentration PPDD for 48 h survival (b) refers to the estimated NEC while the corresponding comparisons for 96 h (d) and 192 h (f) refer to the LC_{50}. For corresponding graphical representations of the NEC model subsets for the 96 and 192 h assessments refer to Fig. S4. For interpretation of the references to colour in this figure legend, the reader is referred to the web version of this article.

HFO WAF exposure. Average larval survival was high in seawater controls at the end of the 48 h exposure period (96%) and significantly impacted following exposure to increasing TAH concentrations (Fig. 3a). LC_{50} values were similar across light treatments but approximately 1.2-fold lower in the presence of UVR (98% probability of a difference; Fig. 3b, Table 1). UVR co-exposure also lowered the NEC threshold for larval survival 2.3-fold (100% probability; Fig. S5a–b, Table 1). Replicates with 100% mortality were only observed at the highest TAH concentrations applied (788 and 760 µg L^{-1} TAH +UVR and −UVR, respectively; Fig. 3a), and at these concentrations many larvae appeared as white, immobile larva-shaped masses of lysed cells (Fig. 4f).

The occurrence of deformed (Fig. 4d–e) and very small to small (10–600 µm; Fig. 4e) larvae at the end of the 48 h exposure increased with increasing TAH concentration (Fig. 3c, Table 1), sometimes leading

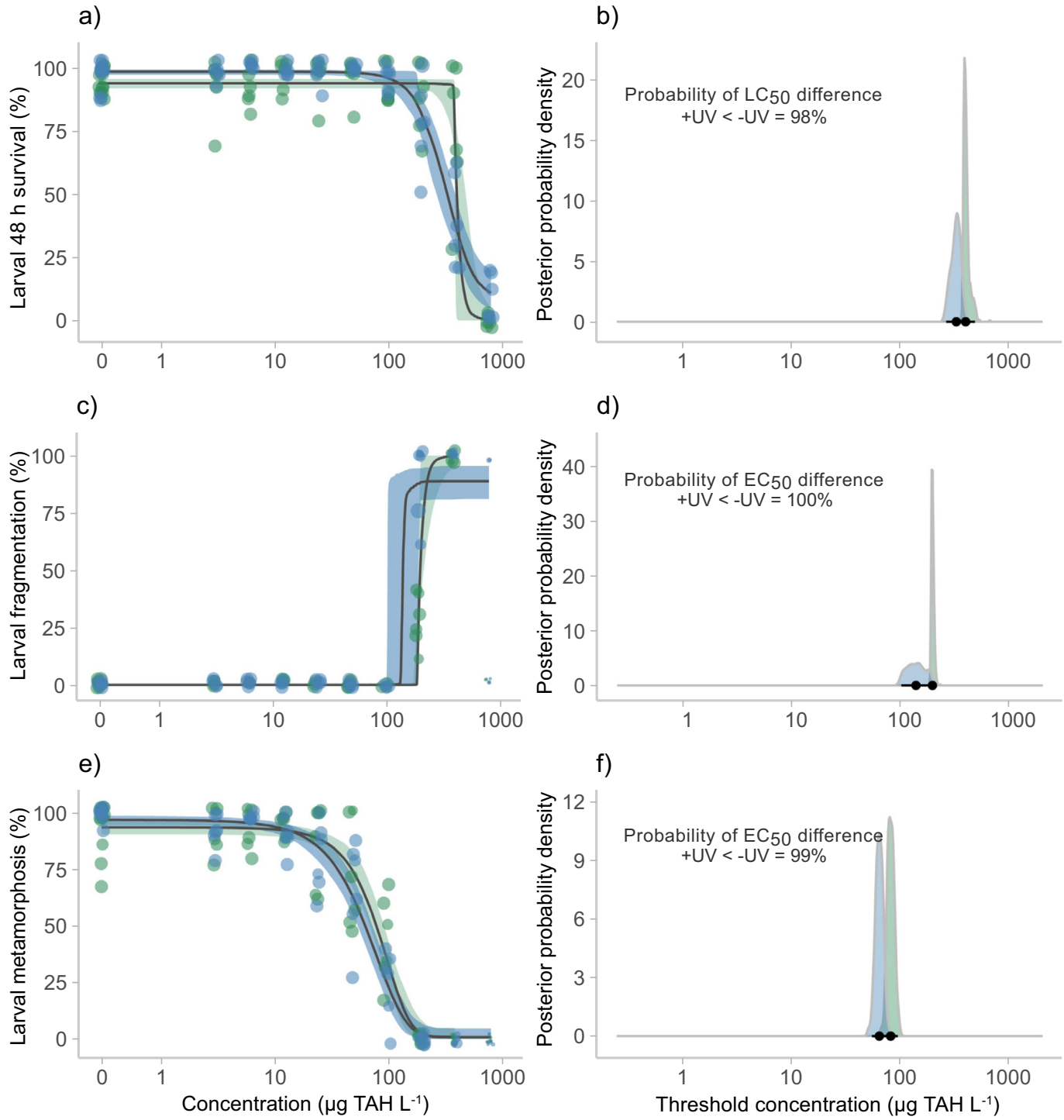

Fig. 3. *A. millepora* larval survival (a), occurrence of small larvae (c) and metamorphosis success (e) following exposure to HFO WAFs under visible light in the absence (green; −UVR) or presence (blue; +UVR) of UVR, and PPDD for derived LC_{50} (b) and EC_{50} (d and f) values. Model median (solid line), 95% credible intervals (shaded band) and raw data points (circles) shown for each assessment. PPDD median (solid dot) and 95% credible intervals (solid line) shown for LC/EC_{50}. Data from larval assay performed in December of 2017. For corresponding graphical representations of the NEC model subset refer to Fig. S4. For interpretation of the references to colour in this figure legend, the reader is referred to the web version of this article.

to an increase in the total number of larvae relative to the start of exposure (Fig. 5a). These smaller larvae (Fig. 4e) were determined to be generated via the fragmentation of normal sized, originally healthy larvae (Fig. 4a) that developed abnormalities, became severely deformed (Fig. 4d) and finally fragmented. Deformations observed in the larvae pre-fragmentation included holes, bends, lumps and areas of necrotic tissue, with some larvae noted to have lumps of similar shape and size as the smaller larvae (Fig. 4e). The undersized larvae retained the ability to swim: from spinning in one place to traversing the entirety of the well. Small larvae occurred at lower concentrations in the presence of UVR resulting in a 1.4-fold decrease in the EC_{50} (100% probability; Fig. 3d). Additional small and very small larvae were observed at the end of the 24 h metamorphosis incubation period relative to the 48 h assessment (Fig. 5b), and for some replicates, all larvae of normal shape and length (~1000 µm) had disappeared by the time of metamorphosis assessment (>190 and

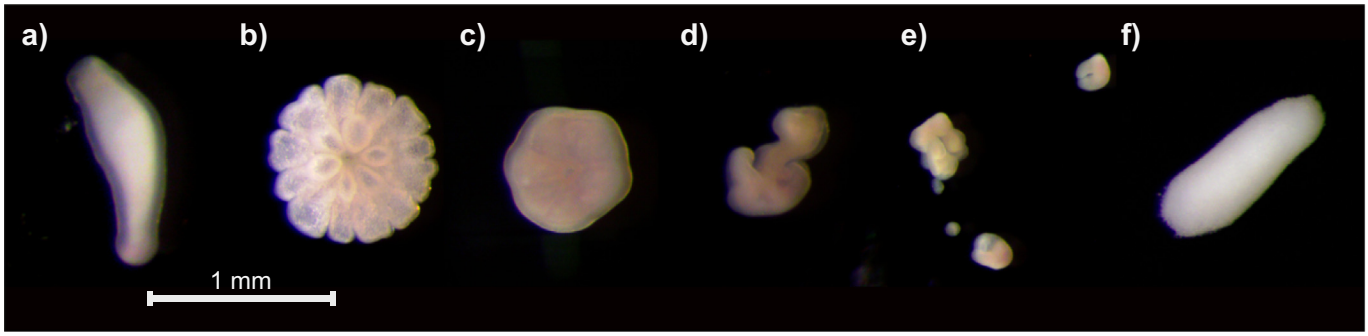

Fig. 4. Examples of normal and abnormal larvae and recruits observed during larval *A. millepora* assay. Morphologies observed included: a) normal sized planula larva (0–100 μg L^{-1} TAH), b) fully metamorphosed recruit (0–100 μg L^{-1} TAH), c) early stage metamorphosed recruit (10–500 μg L^{-1} TAH), d) severely deformed larva undergoing fragmentation (10–500 μg L^{-1} TAH), e) swimming larval fragments and deformed larvae undergoing fragmentation (10–500 μg L^{-1} TAH) and f) larva-shaped mass of dead cells (>350 μg L^{-1} TAH). Treatment concentrations where each morphology was observed shown in brackets. Examples extracted from photographs obtained using a Leica MS5 dissecting microscope with a 5.1 Mp camera calibrated using the ToupView software.

370 μg L^{-1} +UVR and −UVR, respectively). Fragmentation occurred at lower TAH concentrations in the presence of UVR (Fig. 3c, Table 1, Fig. S5c–d) but fragments appeared to survive longer in the absence of UVR. Similar observations were made during the preliminary larval experiment performed using larvae originating from Falcon Island (Figs. 5b and S7, Table S13).

Larval metamorphosis success was significantly reduced by exposure to HFO WAF at low TAH concentrations both in the absence and presence of UVR (Figs. 3e and S5e). Metamorphosis was the most sensitive larval endpoint assessed for both light treatments (Fig. 3, Table 1). UVR co-exposure resulted in a 1.3-fold reduction of the metamorphosis EC_{50} (99% probability; Fig. 3e–f) and a 2.1-fold reduction of the NEC (100% probability; Fig. S5e–f). While metamorphosis was still observed at mid-high concentrations (<190 μg L^{-1}) recruits were generally underdeveloped or failed to undergo complete metamorphosis (Fig. 4c), with first observations of underdeveloped recruits occurring at low-mid concentrations (>50 μg L^{-1}). Small and very small larvae did not generally undergo metamorphosis, but the first phase of metamorphosis, attachment to the substrate, was sometimes observed. No metamorphosis was observed at high TAH concentrations (>200 μg L^{-1}) regardless of light treatment (Fig. 3e).

3.5. Putative CTLBB estimation

Putative CTLBBs calculated from the EC_{50} and LC_{50} values (in the absence of UVR) were very low, ranging from 4.4 μmol g^{-1} octanol for *A. millepora* larval metamorphosis to 21.6 μmol g^{-1} octanol for larval survival (Table 1). CTLBBs were not calculated if an EC_{50} or LC_{50} was not reached, or for UVR treatments as the observed toxicity would most likely be a combination of narcosis and phototoxicity. The derived CTLBBs for assessed endpoints all fall within the 10% most sensitive species, when compared to the 79 mostly aquatic species currently included in the TLM database (McGrath et al., 2018). Additionally, the three most sensitive endpoints assessed here (larval metamorphosis success, fertilisation success at low sperm densities and latent embryonic survival) are equally or more sensitive than the most sensitive species in the database (Table 1).

4. Discussion

4.1. Overarching trends/summary

HFO WAF exposure negatively impacted all early life stages of *A. millepora* tested, with UVR co-exposure generally increasing the direct effects of HFO. The order of sensitivity (highest to lowest), based on EC/LC_{50} in the absence of UVR, was: (i) larval metamorphosis; (ii) fertilisation at low sperm densities; (iii) latent embryo survival ≥96 h; (iv) larval fragmentation; (v) larval survival; (vi) fertilisation at optimal sperm densities; and (vii) 48 h embryo survival. The strong latent effects of dissolved aromatics on embryo survival indicate the potential for short exposure assays (without post-exposure monitoring) to underestimate toxicity thresholds, and latent effects should be investigated further in other early life stages. In addition to being the most sensitive early life stage tested, quantification of larval metamorphosis was unaffected by confounding factors, which can affect and/or mask toxicity, including sperm density (fertilisation assay) and fragmentation (embryo and larval assays). Larval metamorphosis was approximately 5-fold more sensitive to HFO WAF than survival, but failure to metamorphose from a larva to a juvenile polyp represents an equally important impact on coral recruitment. Therefore, metamorphosis success is an appropriate toxicity endpoint for deriving toxicity thresholds for oil spill risk assessments. The derivation of putative CTLBB values allowed direct comparison of sensitivity between some endpoints for these early coral life stages and the 79 aquatic species in the TLM narcotic toxicity database, which is used as a basis to model toxicity thresholds of oils from their composition alone (McGrath et al., 2018). Based on the putative CTLBBs, metamorphosis of *A. millepora* larvae is more sensitive than the most sensitive species currently included in the TLM database (*Melanotaenia fluviatilis*, 9 μmol g^{-1} octanol; McGrath et al. (2018)). This further indicates its sensitivity to dissolved aromatics and highlights the value of developing more robust CTLBBs for the early life stages of coral, which can contribute to improving tropical toxicity modelling. Exposure to relatively low UVR intensities increased HFO WAF toxicity between 1.2- (larval LC_{50}) and 94-fold (fertilisation EC_{10} at 10^6 sperm mL^{-1}) across the assessed life stages and endpoints. On average, the end of exposure EC/LC_{50} for embryonic and larval endpoints decreased by 1.3-fold, with 2.0- and 2.6-fold decreases observed for EC/LC_{10} and NEC compared to −UVR treatments. The influence of UVR co-exposure on the toxicity of HFO WAF to all early life stages highlights the need for further studies to quantify phototoxicity across a full range of UVR intensities that are relevant for species living in clear, shallow-water coral reef environments.

4.2. Fertilisation

The sensitivity of fertilisation to dissolved HFO aromatics varied considerably with sperm density and light exposure. Fertilisation success in seawater controls, regardless of light treatment applied, were in line with those previously reported for *A. millepora* in the absence of light (Willis et al., 1997; Ricardo et al., 2015). However, direct comparisons with previous studies on the effects of dissolved aromatics on coral fertilisation are difficult due to differences in methodologies, oil compositions and units of reporting used. Nevertheless, the relative insensitivity of fertilisation success of *A. millepora* gametes exposed to a HFO WAF at optimal-high sperm densities in the dark is consistent with previous reports. The same species exposed to crude oil WAF at 10^6 sperm mL^{-1},

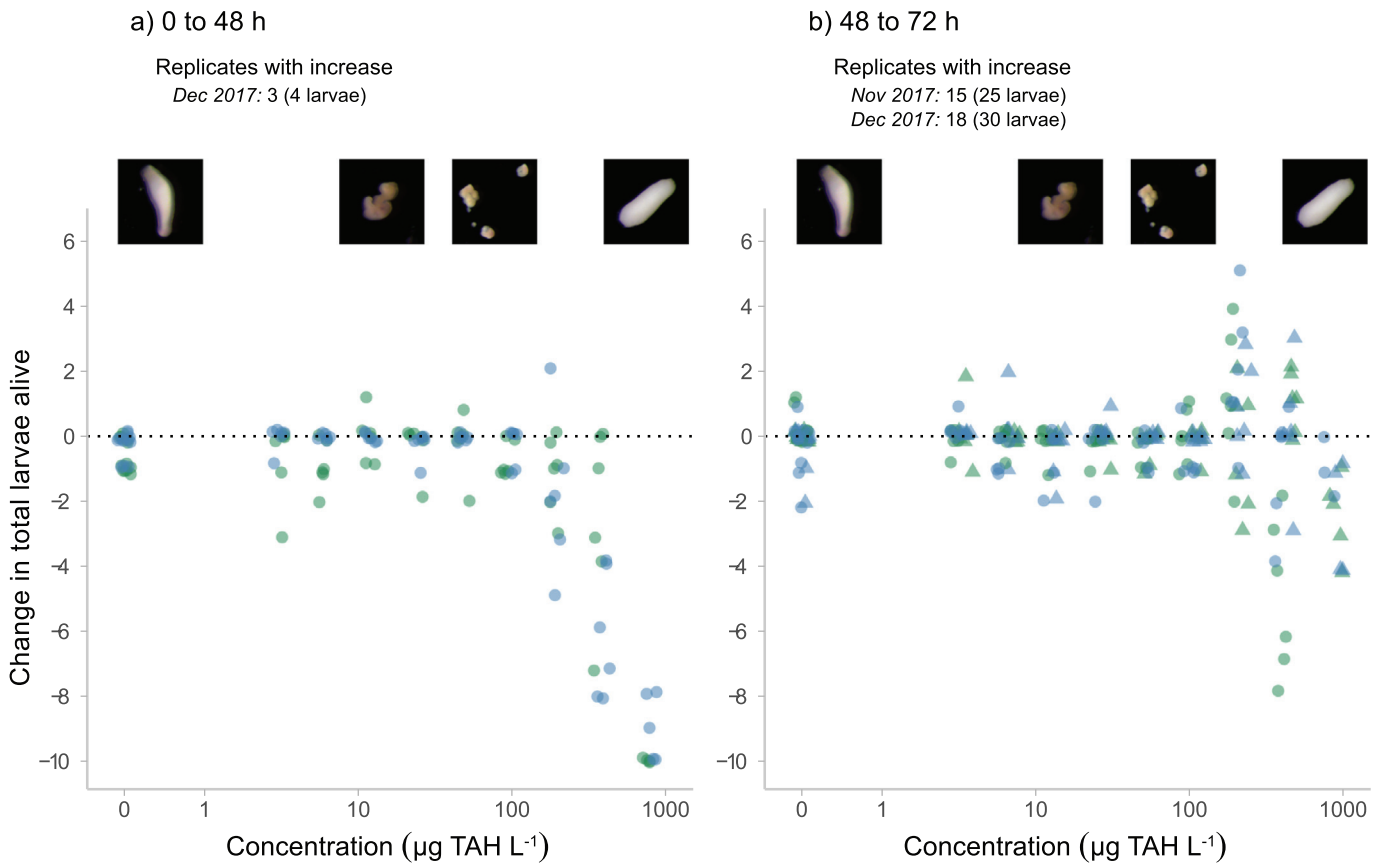

Fig. 5. Change in total number of *A. millepora* larvae and recruits alive between start and end of exposure (a) and between induction of metamorphosis and metamorphosis assessment (b) under visible light in the presence (blue) or absence (green) of ultraviolet radiation. Data from preliminary larval survival and metamorphosis assay performed in November (triangles) and larval survival and metamorphosis assays performed in December (circles) of 2017.

reported no effects at 165 µg L^{-1} TRH (determined by UV fluorescence; Negri and Heyward (2000)). However, the same study reported a ~20% reduction in fertilisation for *A. millepora* when exposed to 180 µg L^{-1} TRH from produced formation water at the same high sperm densities. Inhibition of fertilisation success in *Acropora microphthalma* (38% reduction) was also observed when exposed to mineral lubricating oil WAF concentrations ≥200 µg L^{-1} TRH at 10^6 sperm mL^{-1} (Mercurio et al., 2004). While there is mounting evidence that coral fertilisation is relatively insensitive to dissolved aromatics at optimal or high sperm densities, there was >10-fold increase in the sensitivity of *A. millepora* fertilisation (based on NEC/EC_{10}s) to HFO WAF at low sperm densities (10^3 sperm mL^{-1}), making it one of the most sensitive endpoints assessed in the present study.

Fertilisation assays performed on corals and other invertebrates have also shown increased sensitivity to pollutants at sub-optimal sperm densities (Marshall, 2006; Hollows et al., 2007; Ricardo et al., 2018). The current study identified abnormal embryonic development and cell lysis following exposure to dissolved aromatics, supporting previous findings (Harrison, 1994; Harrison, 1999; Mercurio et al., 2004). However, the high dependence of toxicity on sperm density suggests sperm may be more affected than eggs (Ricardo et al., 2018). The sensitivity of fertilisation toxicity thresholds to variations in sperm density raises concerns for their application in risk assessments as sperm densities in situ are not well known. For example, fertilisation success in the field is reported to vary between 0 and 90% in the first 2 h after gamete release (Oliver and Babcock, 1992; Levitan et al., 2004), indicating sub-optimal sperm densities frequently occur. Furthermore, fertilisation success is highly dependent on the environmental conditions (wind, currents, sediments, bleaching, asynchrony) during the spawning event, which affect both sperm densities and the likelihood of encounters with eggs of conspecifics (Omori et al., 2001; Hollows et al., 2007; Ricardo et al., 2015; Shlesinger and Loya, 2019). Although the sensitivity of coral fertilisation to HFO varies with sperm density, coral gametes concentrated at or near the surface have the potential to be exposed to the highest concentrations of dissolved aromatics following a surface spill (NRC, 2003). Furthermore, the impacts of direct contact between positively buoyant coral eggs and oil droplets or slicks should also be considered. This has not been investigated to date and has the potential to further decrease fertilisation success and thereby recruitment.

4.3. Embryonic development

The present study is the first to demonstrate negative impacts of dissolved aromatics from petroleum products on coral embryos. Previous studies exposing embryos of the mussel *Mytilus galloprovincialis* and the sea urchin *Paracentrotus lividus* to marine fuel oil WAF for 48 h also showed negative impacts, with developmental stage and larval growth EC_{50}s of 82% and 45% WAF, respectively (Bellas et al., 2013). Exposure of coral embryos to other pollutants can also cause embryo mortality; for example, *Acropora tenuis* embryos (12 hpf) exposed to coal dust for 72 h exhibited up to 26% higher mortality than seawater controls (Berry et al., 2017). The potential for latent effects on embryos was also evident for *A. tenuis* (8 hpf) exposed to suspended sediments or elevated nutrients, which showed limited effect on survival at the end of a 28 h exposure, but significantly reduced settlement following recovery in clean seawater (Humanes et al., 2017). Latent oil toxicity-induced mortality has also been observed for other coral life stages including larvae of *Orbicella faveolata* and *Agaricia humilis*, where mortality was only observed during the post-exposure period (Hartmann et al., 2015). Similarly, latent impacts were observed on the growth of *Seriatopora hystrix*, *Seriatopora guttatus*

and *Stylophora pistillata* juveniles exposed to gas condensate WAF for 96 h while larvae or newly settled recruits (Villanueva et al., 2008). These reports support the findings of the present study that latent impacts may outweigh the impacts observed at the end of exposure, and that ignoring latent effects may lead to significant underestimation of toxicity thresholds.

Embryonic survival was affected by two competing processes: (i) mortality from exposure to dissolved aromatics and (ii) embryo fragmentation. This fragmentation caused an apparent increase in embryo numbers in many treatments and resulted in the embryo survival metric representing the "net" outcome of these processes combined. Embryo fragmentation due to physical disturbances has previously been documented for acroporid corals and can produce fully viable larvae in the absence of other stressors (Heyward and Negri, 2012). Embryo fragmentation masked mortality in this assay by increasing apparent numbers of embryos, which resulted in high net survival at 48 h, even at high TAH concentrations. In contrast, latent survival of embryos was significantly affected by exposure to dissolved aromatics with a strong concentration-response observed regardless of light treatment. The latent impacts decreased LC_{50} values by 2.9 to 5.4-fold compared to the end of exposure (48 h) but did not vary substantially between the two assessment times (96 and 192 h). Latent mortality due to oil toxicity clearly overcame the increased embryo numbers, resulting from fragmentation during exposure, after embryos/larvae were transferred to clean FSW. The smaller larvae resulting from fragmented embryos may also have been more susceptible to the effects of the dissolved aromatics as resources and lipids were split across two or more larvae (Okubo et al., 2017) and the surface-area-to-volume ratio increased (Pelletier et al., 1997). During an oil spill, buoyant embryos are likely to be simultaneously exposed to the oil slick/droplets, the highest dissolved TAH concentrations (NRC, 2003) and turbulence (e.g. from wave action), which also promotes fragmentation (NRC, 2003; Heyward and Negri, 2012). Coral embryos uniquely lack a protective membrane (Heyward and Negri, 2012) and embryos of other invertebrates are therefore unlikely to fragment in the same way. While embryonic development assays are routinely used to assess sensitivity to pollutants for some taxa, and have been suggested as a high-throughput alternative to assays using adults (Capela et al., 2020), the possibility of fragmentation renders net embryonic survival of coral embryos a less reliable endpoint for application in risk assessments.

4.4. Planula larvae

A. millepora larvae were significantly impacted by HFO WAF exposure both in the presence and absence of UVR. Larval metamorphosis was inhibited at the lowest TAH concentrations (>21.2 μg L^{-1} TAH), higher concentrations (>184 μg L^{-1} TAH) also caused larval fragmentation, while larval survival was only affected at the highest TAH concentrations tested (>373 μg L^{-1} TAH).

4.4.1. Metamorphosis

Metamorphosis success was high in seawater controls but decreased with increasing concentration of dissolved hydrocarbons, regardless of light treatment, with no metamorphosis observed at concentrations >200 μg L^{-1} TAH. The sensitivity of metamorphosis success observed here is within range of that previously reported for *A. millepora* larvae exposed to other petroleum products (Negri and Heyward, 2000). *A. millepora* larvae appear to be at least as sensitive to petroleum hydrocarbon exposure as other coral species in the absence of UVR, including *P. astreoides* (Goodbody-Gringley et al., 2013), *A. tenuis* (Negri et al., 2016; Nordborg et al., 2018), *A. humilis* (Hartmann et al., 2015) and *O. faveolata* (Goodbody-Gringley et al., 2013; Hartmann et al., 2015). However, due to differences in the chemical composition of the petroleum products used, and the exposure and analytical methodologies applied, direct quantitative comparisons are of limited significance (Redman and Parkerton, 2015; Hodson et al., 2019).

In addition to inhibition of metamorphosis, partial metamorphosis resulting in underdeveloped recruits also increased at higher TAH concentrations. This partial metamorphosis ranged in severity from incomplete formation of mesenterial septa, characteristic of fully metamorphosed recruits (Heyward and Negri, 1999), to inability to proceed further than attachment to the substrate during the metamorphosis incubation period. Similar observations have previously been made for *Heteroxenia fuscescense* larvae, where attachment but no metamorphosis was observed for larvae exposed to chemically enhanced oil WAF (CEWAF) for 96 h (Epstein et al., 2000). Underdeveloped recruits and delayed settlement was also observed for *A. tenuis* larvae exposed to HFO and diesel WAF (Nordborg et al., 2018). Narcotic toxicity may be responsible for these effects but it has also been suggested that inhibition of metamorphosis may result from the action of dissolved aromatics on specific developmental pathways (Negri et al., 2016). The expression of several stress-related genes has previously been observed in coral larvae (Overmans et al., 2018) and adults (Xiang et al., 2019) exposed to dissolved aromatics, while growth and development-related genes were depressed in soft corals exposed to a mixture of PAHs (Woo et al., 2013). The inclusion of gene expression assays in larvae exposed to dissolved aromatics may clarify the mode of action of aromatics on larval metamorphosis success.

It is unclear whether the *A. millepora* larvae that failed to undergo metamorphosis during the incubation period could recover and potentially attach and complete metamorphosis at a later time, e.g. if transferred to clean seawater. However, Epstein et al. (2000) and Hartmann et al. (2015) both reported that coral larvae exposed to oil WAFs were unable to settle after transfer to clean seawater prior to settlement induction. In this study, the small, fragmented larvae, that were generated at TAH concentrations higher than those that inhibited metamorphosis, may be even less likely to settle than whole larvae as some of the fragments may lack the chemoreceptors required for initiation of settlement (Heyward and Negri, 1999) or genetic regulators of metamorphosis associated with the animal pole (Okubo et al., 2017). Further investigations into the latent impacts of oil exposure on metamorphosis success, the mechanism of action for metamorphosis inhibition, the metamorphosis competency of larval fragments and whether recovery may restore metamorphosis competency are clearly warranted.

4.4.2. Survival and fragmentation of larvae

The sensitivity of coral larval survival appears to vary between species, larval ages and oil pollutants tested, with some larvae experiencing no mortality while others show potentially higher sensitivity than the *A. millepora* larvae assessed here. However, due to inconsistencies in the analytical and exposure methodologies used, as well as a lack of chemical analysis for several previous studies, quantitative comparisons of larval sensitivities are not valid (Redman and Parkerton, 2015; Turner and Renegar, 2017; Hodson et al., 2019). Nevertheless, if the derived threshold concentrations for *A. millepora* are expressed as TRH (e.g. LC_{10} 1039 and LC_{50} 1103 μg L^{-1}) then *A. millepora* appears to be more sensitive to petroleum hydrocarbons (lower LC_{10} or LC_{50}) than larvae of *A. tenuis*, *Platygyra sinensis* and *Coelastrea aspera* (previously Goniastrea; Lane and Harrison (2000)), *S. pistillata* (Epstein et al., 2000; Villanueva et al., 2008), *Pocillopora damicornis* and *Pocillopora verrucosa* (Villanueva et al., 2008). Larvae of the following species may be more sensitive than *A. millepora*: *O. faveolata* (Goodbody-Gringley et al., 2013; Hartmann et al., 2015), *A. humilis* (Hartmann et al., 2015) and *Porites astreoides* (Goodbody-Gringley et al., 2013).

The observed fragmentation of larvae may have been due to narcotic toxicity, with aromatics concentrating in and disrupting cell membranes. At high concentrations, the structural membranes may have failed altogether, generating fragments, some of which are able to continue swimming. Larval abnormalities and tissue degeneration have been observed for *S. pistillata* larvae exposed to CEWAF of Egyptian oil (Epstein et al., 2000). The authors reported that deformed larvae were observed to release "small spherical bodies, (probably lipid droplets)"

and to lose their normal swimming behaviour, in addition to settlement inhibition (Epstein et al., 2000). Following histological comparisons, the authors concluded that CEWAF exposure had damaged the ectodermal outer layer. In larvae of the soft coral *H. fuscescense*, exposure to the same Egyptian oil CEWAFs also caused deformation of larvae ("ball-like deformed structure") (Epstein et al., 2000). Morphological deformations were also observed in *A. tenuis* larvae exposed to HFO and diesel WAF (Nordborg et al., 2018) as well as those exposed to solutions containing anthracene or phenanthrene (Overmans et al., 2018). It is unclear whether the reports by Epstein et al. (2000) describe the same fragmentation process observed in the present study, in particular as the dispersant may have been the main causative agent, but the spherical/"ball-like" appearance is consistent with the small and very small larvae observed here. While it is unclear whether larval fragments have a comparable viability, or competency for metamorphosis as whole larvae, they retained at least partial ability to swim. As for embryos, the fragmentation of larvae results in an underestimation of the impacts of HFO WAF on larval survival as the number of new, swimming fragmented larvae may be larger than the number of whole larvae and fragments that die during a given period. Additionally, many of the small and very small larvae observed at the end of the 48 h exposure had died and dissolved by the end of the metamorphosis incubation period (at 72 h), making quantification of net larval survival even less reliable. This result further supports the use of larval metamorphosis success as the primary endpoint investigated when testing the toxicity of dissolved aromatics towards coral larvae.

4.5. Phototoxic effects on the early life stages of coral

Co-exposure to UVR affected all early coral life stages and endpoints assessed in this study. Phototoxicity causes damage to cellular structures or genetic material and occurs when dissolved aromatics are exposed to UVR, or short wavelength visible light, through two main pathways: photosensitisation or photomodification/photooxidation. *Photosensitisation* results in production of reactive oxygen species, as photo-excited aromatics decay back to their ground states, while *photomodification* results in the production of more reactive photoproducts or intermediates from parent aromatics, often through oxidation (Barron, 2017).

Co-exposure to light increased the effects of HFO WAF on *A. millepora* fertilisation success, with exposure to UVR resulting in >70-fold reductions of all threshold concentrations (NEC, EC_{10} and EC_{50}). Interestingly, the presence of visible light alone also led to a reduction of threshold concentrations by 1.2- to 1.9-fold, indicating light in the 400–700 nm range may also play a subtle role in increasing the effects of dissolved aromatics on fertilisation. There was no apparent effect of UVR on fertilisation success in the absence of dissolved aromatics, indicating that the applied UVR intensity may have been too low to cause damage to sperm or inhibit fertilisation (Dahms and Lee, 2010). However, phototoxic effects on fertilisation was apparent at very low TAH concentrations and is likely to primarily impact sperm, which unlike eggs, do not contain UVR-protective mycosporine-like amino acids (Dunlap and Shick, 1998). Nevertheless, broadcast spawning corals such as *A. millepora* generally spawn at night, so phototoxicity would not increase the vulnerability of gametes for this species in situ. However, the fertilisation of some reef-building corals that also spawn during the day (Bouwmeester et al., 2011; Bronstein and Loya, 2011; Schmidt-Roach et al., 2012; Suzuki, 2012) may be vulnerable to phototoxicity.

UVR increased the immediate impacts on embryonic survival (at 48 h) but this increase was small compared to the latent mortality, which occurred after transfer to clean FSW. Indeed, the generation of small embryo and larval fragments during the 48 h exposure confounded the embryo survival data (as described above). Fragmentation rates in the presence of UVR were potentially higher (not possible to assess), which may have increased the apparent survival, thereby masking toxicity. Further studies should investigate the effect of UVR on embryo fragmentation under a range of turbulence and UVR intensities to increase certainty of the influence of phototoxicity on coral embryos.

A. millepora larval metamorphosis EC_{50} was 1.3-fold lower in the presence of UVR while the EC_{10} was reduced by ~1.6-fold. Similar phototoxicity was previously observed for *A. tenuis* larvae (1.6- to 1.9-fold lowering of metamorphosis threshold concentrations) exposed to the same oil using the same exposure methodology (Nordborg et al., 2018). The *A. tenuis* metamorphosis EC_{50} +UVR (51 μg TAH_{35} L^{-1}) was lower than that observed for *A. millepora* in the present study, but the EC_{50} −UVR was lower for *A. millepora* than *A. tenuis* (96 μg TAH_{35} L^{-1}). While threshold concentrations were similar across the two studies, phototoxicity was more apparent in *A. tenuis* larvae, highlighting the potential for species-specific sensitivities to phototoxicity. Such differences may be due to differences in the protection from UVR by mycosporine-like amino acids (Dunlap and Shick, 1998).

Tropical, shallow-water coral reefs occur in geographic regions experiencing high UVR intensities throughout the year. UVR irradiance at or just below the surface on the central GBR was measured at 5.98–6.28 mW cm^{-2} UVA and 0.323 mW cm^{-2} UVB (for further details refer to Fig. S9 and Table S14) in the lead up to the annual mass-spawning events in 2017 (generally November–December for mid-shelf reefs on the central GBR; Babcock et al. (1986)). While UVR applied in the present study caused a substantial increase in the direct toxicity of HFO, the total UVR intensity applied was low compared to the potential exposure of buoyant embryos and larvae at the water surface or in clear, shallow water (<22% total UVA and UVB of surface irradiance). Additionally, a lower percentage of the total irradiance from the UVR lights used in the present study consisted of the higher energy, UVB radiation (2% compared to 5%; Tables S3 and S14). Phototoxicity increases markedly with increases in UVR intensity and is dependent on the spectrum (Barron, 2017); hence, the phototoxicity of HFO towards developing coral embryos and coral larvae in the field is likely to be underestimated in the present study. To ensure threshold concentrations for oil toxicity applied in risk assessments are representative of conditions in situ, further research on the impacts of dissolved aromatics to coral larvae under different UVR intensities, and spectral profiles, should be undertaken.

4.6. Putative CTLBB estimates

Comparison of sensitivity to oil exposure across species or endpoints is often required for risk assessments but is confounded by differences in oil composition, solution preparation and exposure methodology. As a result, the direct comparison of threshold concentrations (e.g. μg L^{-1}) is discouraged and alternative methods of comparison should be used (Redman et al., 2012; Redman and Parkerton, 2015). The comparison of species-specific CTLBBs is the most effective method to rank species sensitivity to aromatic hydrocarbon exposure, where low CTLBBs indicate more sensitive species regardless of oil composition (Di Toro et al., 2000; French-McCay, 2002; Redman and Parkerton, 2015).

As expected, the putative CTLBB values for each early life stage followed the same order of sensitivity as the EC_{50}s expressed in μg L^{-1} TAH (Table 1). However, the derivation of putative CLTBBs allowed the most valid ranking of sensitivity among these life stages as it also accounted for the small differences in WAF composition between assays. CTLBBs were not reported for assays where UVR was applied as the TLM cannot account for the potential contribution of phototoxicity to the observed results, including for the presence of potential photooxidation products in WAFs. The putative CLTBBs derived here indicate that *A. millepora* larval metamorphosis is more sensitive than the 79 species in the TLM database. All assessed endpoints where a CTLBB could be derived were substantially more sensitive than the geometric

mean species sensitivity of the TLM database (71.1 μmol g^{-1} octanol) and within the 10th percentile of most sensitive species currently included (McGrath et al., 2018). The few CTLBB values previously published for corals, including the 51.6 μmol g^{-1} octanol definitive CTLBB for adults of the cold-water coral *Lophelia pertusa* (Bytingsvik et al., 2020) and preliminary CTLBBs (based on LC_{50} responses to a single PAH) of 199–698 μmol g^{-1} octanol for three Atlantic scleractinian corals (Renegar and Turner, 2021), are also substantially higher than the putative CTLBBs derived here. The derivation of definitive CTLBBs for metamorphosis in coral larvae, by performing assays using individual aromatic compounds (French-McCay, 2002; Redman et al., 2012), should be prioritised as a valuable contribution to the TLM database as it is currently comprised predominantly of temperate (~90%) and/or freshwater (~60%) species (McGrath et al., 2018). A definitive CTLBB for larval metamorphosis would improve confidence that hazard concentration thresholds (e.g. HC5) calculated using models such as PETROTOX (Redman et al., 2012; Redman et al., 2017) are also protective of these sensitive early life stages of keystone tropical coral reef taxa.

5. Conclusion

Heavy fuel oil negatively affected *A. millepora* across all early life stages tested with increased toxicity observed in the presence of UVR. HFO affected early life stages of coral at concentrations as low as 21, 103 and 21 μg L^{-1} TAH for fertilisation, embryo survival and larval metamorphosis, respectively (Table 1). These concentrations are below those that have been reported in the field after spills (Diercks et al., 2010; Baum et al., 2016), indicating *A. millepora* recruitment is likely to be impacted if oil spills were to coincide with annual spawning events; both during spawning nights as well as during larval development and settlement in the weeks following spawning. Embryo and larval survival were relatively insensitive to low TAH concentrations and effectively quantifying these endpoints was confounded by fragmentation. While fertilisation could be very sensitive to aromatics, this sensitivity was highly dependent on sperm densities (which are largely unknown during in situ spawning events). In contrast, larval metamorphosis was both sensitive to oil exposure at low concentrations and unaffected by fragmentation. Furthermore, metamorphosis of planula larvae into sessile coral polyps represents a critical lifecycle bottleneck for reef-regeneration following disturbances (Randall et al., 2020) and has been shown to be a robust and replicable assay for the toxicity of dissolved aromatics to coral (Epstein et al., 2000; Negri and Heyward, 2000; Villanueva et al., 2008; Goodbody-Gringley et al., 2013; Hartmann et al., 2015; Negri et al., 2016; Nordborg et al., 2018; Overmans et al., 2018). Therefore, the toxicity thresholds for metamorphosis success are recommended as the most relevant for application in oil spill risk assessments of the early life stages tested in this study.

Coral metamorphosis was also sensitive to dissolved aromatics in comparison to other aquatic species, as demonstrated by its low putative CTLBB. The putative metamorphosis CTLBB places *A. millepora* as the most sensitive species and endpoint assessed to date when compared to the TLM database (Redman et al., 2017; McGrath et al., 2018). Larval metamorphosis is likely to be more sensitive to dissolved aromatics than endpoints for adult corals (Turner and Renegar, 2017; Nordborg et al., 2020), with the only reliable available data being for adults of *Porites divaricata* with an EC_{50} of 7442 μg L^{-1} for 1-methylnaphthalene (Renegar et al., 2017). However, further studies to derive definitive CTLBBs for coral larvae, as well as juvenile and adult corals, are required to confirm their relative sensitivity. This would enable the incorporation of these keystone coral reef taxa into TLM databases for toxicity models such as PETROTOX (Redman et al., 2012; McGrath et al., 2018) and OilToxEx (French-McCay, 2002), enabling the application of predictive toxicity modelling for all oils and petroleum products relevant to reef environments.

The marked increase in toxicity of HFO WAF to *A. millepora* embryos in the days following the end of exposure suggests the typically short, traditional ecotoxicity tests performed with aromatics on early life stages may underestimate sensitivity. Further studies are needed to determine if fertilisation, larval metamorphosis and later life stages of coral are also affected at lower TAH concentrations when monitoring extends beyond the end of exposure. Finally, the application of UVR co-exposure is strongly recommended for future investigations of the impacts of dissolved aromatics on early coral life stages. In the present study, impacts increased across all endpoints assessed at end of exposure, supporting existing evidence of phototoxicity across life stages in several other reef-building coral species (Peachey and Crosby, 1995; Guzmán Martínez et al., 2007; Negri et al., 2016; Nordborg et al., 2018; Overmans et al., 2018). Early life stages of marine taxa have long been recognised as the most at risk for phototoxicity but the likelihood of high UVR co-exposure, and therefore the risk of phototoxicity, has generally been deemed low (McDonald and Chapman, 2002; Barron, 2017). As high intensity UVR co-exposure is highly likely during any oil spill in coral reef environments (Nordborg et al., 2020), accounting for phototoxicity will be critical to ensure risk assessments do not underestimate the hazards posed by oil pollution to early coral life stages. Recent risk assessments associated with the Deep Water Horizon spill have also recognised the potential effects of phototoxicity on shallow ecosystems (<20 m depth) and proposed a blanket 10-fold reduction in toxicity thresholds as an interim solution (French-McCay et al., 2018). Further toxicity studies applying relevant UVR intensities are required to refine phototoxic oil toxicity thresholds and ensuring their appropriate application in risk management for coral reefs.

Data statement

Data is available via the Australian Institute of Marine Science data portal (AIMS, 2021) and the scripts used in statistical analysis and visualisation of results are available from GitHub (https://github.com/MNordborg/Nordborg-et-al.-2021-Early-LS-HFO).

Funding sources

Funding for the work presented here was provided by the Australian Institute of Marine Science (Australia), King Abdullah University of Science and Technology (Saudi Arabia), the Australian Government Research Training Program Fee Offset and the AIMS@JCU Scholarship program James Cook University (Australia).

CRediT authorship contribution statement

F. Mikaela Nordborg: Conceptualization, Methodology, Investigation, Data curation, Formal analysis, Visualization, Writing – original draft, Writing – review & editing. **Diane L. Brinkman:** Methodology, Investigation, Formal analysis, Writing – review & editing. **Gerard F. Ricardo:** Methodology, Formal analysis, Writing – review & editing. **Susana Agustí:** Conceptualization, Funding acquisition, Writing – review & editing. **Andrew P. Negri:** Conceptualization, Funding acquisition, Methodology, Validation, Supervision, Writing – original draft, Writing – review & editing.

Declaration of competing interest

The authors declare that they have no known competing financial interests or personal relationships that could have appeared to influence the work reported in this paper.

Acknowledgements

The authors acknowledge the Traditional Owners of the land and sea country where this research was conducted and from which the parent

corals originated, the Wulgurukaba, Bindal and Woppaburra peoples. We pay our respect to their Elders, past, present and emerging, and acknowledge their continuing spiritual connection to their land and sea country. The authors also thank the staff of the National Sea Simulator at the Australian Institute of Marine Science Townsville, QLD, for their technical support and expertise; Florita Flores for her advice regarding the experimental assays; Dr Rebecca Fisher for her advice regarding the statistical analysis; Dr Carly Randall and her team for the collection of parent corals; Tristan Lever, Dr Katarina Damjanovic, Christopher Brunner, Christina Langley, Camille Streel, Edith Strecker, Laura Zeuthen, Roy Borg and Alicia Castle for their time and assistance in performing the experimental work.

Appendix A. Supplementary data

Supplementary data to this article can be found online at https://doi.org/10.1016/j.scitotenv.2021.146676.

References

AIMS, 2021. Petroleum oil sensitivity in the coral *Acropora millepora*: early life stages. Australian Institute of Marine Science. https://apps.aims.gov.au/metadata/view/7b882ea1-f70a-4a02-9b20-02f9d7db9b2c.

Asariotis, R., Premti, A., 2020. Mauritius oil spill highlights importance of adopting latest international legal instruments in the field. https://unctad.org/en/pages/newsdetails.aspx?OriginalVersionID=2451. (Accessed 27 August 2020).

Aurand, D., Coelho, G., 2005. Cooperative aquatic toxicity testing of dispersed oil and the chemical response to oil spills. Ecological Effects Research Forum (CROSERF). Inc. Lusby, MD., Technical Report. vol. 07-03, p. 105.

Babcock, R.C., Bull, G.D., Harrison, P.L., Heyward, A.J., Oliver, J.K., Wallace, C.C., et al., 1986. Synchronous spawnings of 105 scleractinian coral species on the Great Barrier Reef. Mar. Biol. 90, 379–394. https://doi.org/10.1007/BF00428562.

Baird, A.H., Guest, J.R., Willis, B.L., 2009. Systematic and biogeographical patterns in the reproductive biology of scleractinian corals. Annu. Rev. Ecol. Evol. Syst. 40, 551–571. https://doi.org/10.1146/annurev.ecolsys.110308.120220.

Ban, S.S., Graham, N.A.J., Connolly, S.R., 2014. Evidence for multiple stressor interactions and effects on coral reefs. Glob. Chang. Biol. 20, 681–697. https://doi.org/10.1111/gcb.12453.

Banaszak, A., Lesser, M., 2009. Effects of ultraviolet radiation on coral reef organisms. Photochem. Photobiol. 8, 1276–1294. https://doi.org/10.1039/b902763g.

Barron, M.G., 2017. Photoenhanced toxicity of petroleum to aquatic invertebrates and fish. Arch. Environ. Contam. Toxicol. 73, 40–46. https://doi.org/10.1007/s00244-016-0360-y.

Barron, M.G., Ka'aihue, L., 2003. Critical evaluation of CROSERF test methods for oil dispersant toxicity testing under subarctic conditions. Mar. Pollut. Bull. 46, 1191–1199. https://doi.org/10.1016/S0025-326X(03)00125-5.

Baum, G., Kegler, P., Scholz-Böttcher, B.M., Alfiansah, Y.R., Abrar, M., Kunzmann, A., 2016. Metabolic performance of the coral reef fish *Siganus guttatus* exposed to combinations of water borne diesel, an anionic surfactant and elevated temperature in Indonesia. Mar. Pollut. Bull. 110, 735–746. https://doi.org/10.1016/j.marpolbul.2016.02.078.

Bellas, J., Saco-Álvarez, L., Nieto, Ó., Bayona, J.M., Albaigés, J., Beiras, R., 2013. Evaluation of artificially-weathered standard fuel oil toxicity by marine invertebrate embryogenesis bioassays. Chemosphere 90, 1103–1108. https://doi.org/10.1016/j.chemosphere.2012.09.015.

Berry, K.L.E., Hoogenboom, M.O., Brinkman, D.L., Burns, K.A., Negri, A.P., 2017. Effects of coal contamination on early life history processes of a reef-building coral, *Acropora tenuis*. Mar. Pollut. Bull. 114, 505–514. https://doi.org/10.1016/j.marpolbul.2016.10.011.

Birkeland, C., Reimer, A.A., Young, J.R., 1976. Survey of Marine Communities in Panama and Experiments With Oil: US Environmental Protection Agency. Office of Research and Development, Environmental Research Laboratory.

Bouwmeester, J., Berumen, M.L., Baird, A.H., 2011. Daytime broadcast spawning of *Pocillopora verrucosa* on coral reefs of the central Red Sea. Galaxea J. Coral Reef Stud. 13, 23–24. https://doi.org/10.3755/galaxea.13.23.

Bronstein, O., Loya, Y., 2011. Daytime spawning of *Porites rus* on the coral reefs of Chumbe Island in Zanzibar, Western Indian Ocean (WIO). Coral Reefs 30, 441. https://doi.org/10.1007/s00338-011-0733-7.

Bytingsvik, J., Parkerton, T.F., Guyomarch, J., Tassara, L., LeFloch, S., Arnold, W.R., et al., 2020. The sensitivity of the deepsea species northern shrimp (*Pandalus borealis*) and the cold-water coral (*Lophelia pertusa*) to oil-associated aromatic compounds, dispersant, and Alaskan North Slope crude oil. Mar. Pollut. Bull. 156, 111202. https://doi.org/10.1016/j.marpolbul.2020.111202.

Capela, R., Garric, J., Castro, L.F.C., Santos, M.M., 2020. Embryo bioassays with aquatic animals for toxicity testing and hazard assessment of emerging pollutants: a review. Sci. Total Environ. 705, 135740. https://doi.org/10.1016/j.scitotenv.2019.135740.

Dahms, H.-U., Lee, J.-S., 2010. UV radiation in marine ectotherms: molecular effects and responses. Aquat. Toxicol. 97, 3–14. https://doi.org/10.1016/j.aquatox.2009.12.002.

Daley, J., 2019. Month-long oil spill in the Solomon Islands threathens world's largest coral reef atoll. Smart News, Smithsonian Magazinehttps://www.smithsonianmag.com/smart-news/month-long-oil-spill-threatens-world-heritage-site-solomon-islands-180971674/. (Accessed 12 March 2019).

Di Toro, D.M., McGrath, J.A., Hansen, D.J., 2000. Technical basis for narcotic chemicals and polycyclic aromatic hydrocarbon criteria. I. Water and tissue. Environ. Toxicol. Chem. 19, 1951–1970. https://doi.org/10.1002/etc.5620190803.

Di Toro, D.M., McGrath, J.A., Stubblefield, W.A., 2007. Predicting the toxicity of neat and weathered crude oil: toxic potential and the toxicity of saturated mixtures. Environ. Toxicol. Chem. 26, 24–36. https://doi.org/10.1897/06174R.1.

Diercks, A.R., Highsmith, R.C., Asper, V.L., Joung, D., Zhou, Z., Guo, L., et al., 2010. Characterization of subsurface polycyclic aromatic hydrocarbons at the Deepwater Horizon site. Geophys. Res. Lett. 37, L20602. https://doi.org/10.1029/2010GL045046 (1-6).

Dunlap, W.C., Shick, J.M., 1998. Review - ultraviolet radiation-absorbing mycosporine-like amino acids in coral reef organisms: a biochemical and environmental perspective. J. Phycol. 34, 418–430. https://doi.org/10.1046/j.1529-8817.1998.340418.x.

Ellis, J.I., Jamil, T., Anlauf, H., Coker, D.J., Curdia, J., Hewitt, J., et al., 2019. Multiple stressor effects on coral reef ecosystems. Glob. Chang. Biol. 25, 4131–4146. https://doi.org/10.1111/gcb.14819.

Epstein, N., Bak, R., Rinkevich, B., 2000. Toxicity of third generation dispersants and dispersed Egyptian crude oil on Red Sea coral larvae. Mar. Pollut. Bull. 40, 497–503.

Fisher, R., Ricardo, G., Fox, D.R., 2020. jagsNEC: A Bayesian No Effect Concentration (NEC) Package. https://github.com/open-AIMS/NEC-estimation accessed August 26, 2020. doi: https://doi.org/10.5281/ZENODO.3966864.

Forth, H.P., Mitchelmore, C.L., Morris, J.M., Lipton, J., 2017. Characterization of oil and water accommodated fractions used to conduct aquatic toxicity testing in support of the Deepwater Horizon oil spill natural resource damage assessment. Environ. Toxicol. Chem. 36, 1450–1459. https://doi.org/10.1002/etc.3672.

Fox, D.R., 2010. A Bayesian approach for determining the no effect concentration and hazardous concentration in ecotoxicology. Ecotoxicol. Environ. Saf. 73, 123–131. https://doi.org/10.1016/j.ecoenv.2009.09.012.

French-McCay, D.P., 2002. Development and application of an oil toxicity and exposure model, OilToxEx. Environ. Toxicol. Chem. 21, 2080–2094. https://doi.org/10.1002/etc.5620211011.

French-McCay, D., Crowley, D., Rowe, J.J., Bock, M., Robinson, H., Wenning, R., et al., 2018. Comparative risk assessment of spill response options for a deepwater oil well blowout: part 1. Oil spill modeling. Mar. Pollut. Bull. 133, 1001–1015. https://doi.org/10.1016/j.marpolbul.2018.05.042.

Goodbody-Gringley, G., Wetzel, D.L., Gillon, D., Pulster, E., Miller, A., Ritchie, K.B., 2013. Toxicity of Deepwater Horizon source oil and the chemical dispersant, Corexit® 9500, to coral larvae. PLoS One 8, e45574. https://doi.org/10.1371/journal.pone.0045574.

Guzmán Martínez, M.D.C., Romero, P.R., Banaszak, A.T., 2007. Photoinduced toxicity of the polycyclic aromatic hydrocarbon, fluoranthene, on the coral, *Porites divaricata*. J. Environ. Sci. Health A 42, 1495–1502. https://doi.org/10.1080/10934520701480946.

Guzman, H.M., Kaiser, S., Weil, E., 2020. Assessing the long-term effects of a catastrophic oil spill on subtidal coral reef communities off the Caribbean coast of Panama (1985–2017). Mar. Biodivers. 50, 28. https://doi.org/10.1007/s12526-020-01057-9.

Harrison, P., 1994. The effects of oil pollutants on fertilisation rates in the scleractinian coral *Acropora tenuis*. Proceedings of the Joint Scientific Conference on Science, Management and Sustainability of Marine Habitats in the 21st Century. Conference Abstracts. vol. 30.

Harrison, P., 1999. Oil pollutants inhibit fertilization and larval settlement in the scleractinian reef coral *Acropora tenuis* from the Great Barrier Reef, Australia. Sources, Fates and Consequences of Pollutants in the Great Barrier Reef and Torres Strait. Great Barrier Reef Marine Park Authority, Townsville Australia, pp. 8–9 Vol. Conference Abstracts.

Harrison, P.L., Wallace, C.C., 1990. Chapter 7 reproduction, dispersal and recruitment of scleractinian corals. In: Dubinsky, Z. (Ed.), Coral Reefs (Ecosystems of the World; 25). Elsevier Science Publishing Company, New York, pp. 133–207.

Hartmann, A.C., Sandin, S.A., Chamberland, V.F., Marhaver, K.L., de Goeij, J.M., Vermeij, M.J., 2015. Crude oil contamination interrupts settlement of coral larvae after direct exposure ends. Mar. Ecol. Prog. Ser. 536, 163–173. https://doi.org/10.3354/meps11437.

Heyward, A.J., Negri, A.P., 1999. Natural inducers for coral larval metamorphosis. Coral Reefs 18, 273–279. https://doi.org/10.1007/s003380050193.

Heyward, A.J., Negri, A.P., 2012. Turbulence, cleavage, and the naked embryo: a case for coral clones. Science 335, 1064.

Hodson, P.V., Adams, J., Brown, R.S., 2019. Oil toxicity test methods must be improved. Environ. Toxicol. Chem. 38, 302–311. https://doi.org/10.1002/etc.4303.

Hoegh-Guldberg, O., Poloczanska, E.S., Skirving, W., Dove, S., 2017. Coral reef ecosystems under climate change and ocean acidification. Front. Mar. Sci. 4. https://doi.org/10.3389/fmars.2017.00158.

Hollows, C.F., Johnston, E.L., Marshall, D.J., 2007. Copper reduces fertilisation success and exacerbates Allee effects in the field. Mar. Ecol. Prog. Ser. 333, 51–60. https://doi.org/10.3354/meps333051.

Hughes, T.P., Kerry, J.T., Álvarez-Noriega, M., Álvarez-Romero, J.G., Anderson, K.D., Baird, A.H., et al., 2017. Global warming and recurrent mass bleaching of corals. Nature 543, 373–377. https://doi.org/10.1038/nature21707.

Hughes, T.P., Anderson, K.D., Connolly, S.R., Heron, S.F., Kerry, J.T., Lough, J.M., et al., 2018. Spatial and temporal patterns of mass bleaching of corals in the Anthropocene. Science 359, 80. https://doi.org/10.1126/science.aan8048.

Humanes, A., Ricardo, G.F., Willis, B.L., Fabricius, K.E., Negri, A.P., 2017. Cumulative effects of suspended sediments, organic nutrients and temperature stress on early life history stages of the coral *Acropora tenuis*. Sci. Rep. 7, 44101. https://doi.org/10.1038/srep44101.

Jackson, J.B., Cubit, J.D., Keller, B.D., Batista, V., Burns, K., 1989. Ecological effects of a major oil spill on Panamanian coastal marine communities. Science 243, 37. https://doi.org/10.1126/science.243.4887.37.

Jones, R., Ricardo, G., Negri, A., 2015. Effects of sediments on the reproductive cycle of corals. Mar. Pollut. Bull. 100, 13–33. https://doi.org/10.1016/j.marpolbul.2015.08.021.

Labelle, C., Marinier, A., Lemieux, S., 2019. Enhancing the drug discovery process: Bayesian inference for the analysis and comparison of dose–response experiments. Bioinformatics 35, i464–i473. https://doi.org/10.1093/bioinformatics/btz335.

Lane, A., Harrison, P., 2000. Effects of oil contaminants on survivorship of larvae of the scleractinian reef corals *Acropora tenuis*, *Goniastrea aspera* and *Platygyra sinensis* from the Great Barrier Reef. Proceedings of the Ninth International Coral Reef Symposium, Bali. vol. 1, pp. 403–408.

Levitan, D.R., Fukami, H., Jara, J., Kline, D., McGovern, T.M., McGhee, K.E., et al., 2004. Mechanisms of reproductive isolation among sympatric broadcast-spawning corals of the *Montastrea annularis* species complex. Evolution 58, 308–323. https://doi.org/10.1111/j.0014-3820.2004.tb01647.x.

MacNeil, M.A., Mellin, C., Matthews, S., Wolff, N.H., McClanahan, T.R., Devlin, M., et al., 2019. Water quality mediates resilience on the Great Barrier Reef. Nat. Ecol. Evol. 3, 620–627. https://doi.org/10.1038/s41559-019-0832-3.

Marshall, D.J., 2006. Reliably estimating the effect of toxicants on fertilization success in marine broadcast spawners. Mar. Pollut. Bull. 52, 734–738. https://doi.org/10.1016/j.marpolbul.2006.05.005.

McDonald, B.G., Chapman, P.M., 2002. PAH phototoxicity - an ecologically irrelevant phenomenon? Mar. Pollut. Bull. 44, 1321–1326. https://doi.org/10.1016/S0025-326X(02)00358-2.

McGrath, J.A., Di Toro, D.M., 2009. Validation of the target lipid model for toxicity assessment of residual petroleum constituents: monocyclic and polycyclic aromatic hydrocarbons. Environ. Toxicol. Chem. 28, 1130–1148. https://doi.org/10.1897/08-271.1.

McGrath, J.A., Fanelli, C.J., Di Toro, D.M., Parkerton, T.F., Redman, A.D., Paumen, M.L., et al., 2018. Re-evaluation of target lipid model–derived HC5 predictions for hydrocarbons. Environ. Toxicol. Chem. 37, 1579–1593. https://doi.org/10.1002/etc.4100.

Mercurio, P., Negri, A.P., Burns, K.A., Heyward, A.J., 2004. The ecotoxicology of vegetable versus mineral based lubricating oils: 3. Coral fertilization and adult corals. Environ. Pollut. 129, 183–194. https://doi.org/10.1016/j.envpol.2003.11.008.

Negri, A.P., Heyward, A.J., 2000. Inhibition of fertilization and larval metamorphosis of the coral *Acropora millepora* (Ehrenberg, 1834) by petroleum products. Mar. Pollut. Bull. 41, 420–427. https://doi.org/10.1016/S0025-326x(00)00139-9.

Negri, A., Vollhardt, C., Humphrey, C., Heyward, A., Jones, R., Eaglesham, G., et al., 2005. Effects of the herbicide diuron on the early life history stages of coral. Mar. Pollut. Bull. 51, 370–383. https://doi.org/10.1016/j.marpolbul.2004.10.053.

Negri, A.P., Harford, A.J., Parry, D.L., van Dam, R.A., 2011. Effects of alumina refinery wastewater and signature metal constituents at the upper thermal tolerance of: 2. The early life stages of the coral *Acropora tenuis*. Mar. Pollut. Bull. 62, 474–482. https://doi.org/10.1016/j.marpolbul.2011.01.011.

Negri, A.P., Brinkman, D.L., Flores, F., Botte, E.S., Jones, R.J., Webster, N.S., 2016. Acute ecotoxicology of natural oil and gas condensate to coral reef larvae. Sci. Rep. 6, 21153. https://doi.org/10.1038/srep21153.

NEPM, 2013. National Environment Protection (Assessment of Site Contamination) Measure 1999 (ammended 2013), schedule B3 Appendix 1: determination of total recoverable hydrocarbons (TRH) in soil. https://www.legislation.gov.au/Details/F2013C00288/Html/Volume_4#_Toc351712987. (Accessed 12 October 2020).

Nordborg, F.M., Flores, F., Brinkman, D.L., Agustí, S., Negri, A.P., 2018. Phototoxic effects of two common marine fuels on the settlement success of the coral *Acropora tenuis*. Sci. Rep. 8. https://doi.org/10.1038/s41598-018-26972-7.

Nordborg, F.M., Jones, R.J., Oelgemöller, M., Negri, A.P., 2020. The effects of ultraviolet radiation and climate on oil toxicity to coral reef organisms – a review. Sci. Total Environ. 720, 137486. https://doi.org/10.1016/j.scitotenv.2020.137486.

NRC, 2003. Oil in the Sea III: Inputs, Fates, and Effects. National Research Council, The National Academies Press, Washington, DC, p. 277.

Okubo, N., Toshino, S., Nakano, Y., Yamamoto, H.H., 2017. Coral individuality – confluence of change physical splitting and developmental ability of embryos. Sci. Rep. 7, 16006. https://doi.org/10.1038/s41598-017-16273-w.

Oliver, J., Babcock, R., 1992. Aspects of the fertilization ecology of broadcast spawning corals: sperm dilution effects and in situ measurements of fertilization. Biol. Bull. 183, 409–417. https://doi.org/10.2307/1542017.

Omori, M., Fukami, H., Kobinata, H., Hatta, M., 2001. Significant drop of fertilization of *Acropora* corals in 1999: an after-effect of heavy coral bleaching? Limnol. Oceanogr. 46, 704–706. https://doi.org/10.4319/lo.2001.46.3.0704.

Overmans, S., Nordborg, M., Díaz-Rúa, R., Brinkman, D.L., Negri, A.P., Agustí, S., 2018. Phototoxic effects of PAH and UVA exposure on molecular responses and developmental success in coral larvae. Aquat. Toxicol. 198, 165–174. https://doi.org/10.1016/j.aquatox.2018.03.008.

Peachey, R.L., Crosby, D.G., 1995. Phototoxicity in a coral reef flat community. UV Radiation and Coral Reefs, HIMB Technol. Report. vol. 41, pp. 193–200.

Pelletier, M.C., Burgess, R.M., Ho, K.T., Kuhn, A., McKinney, R.A., Ryba, S.A., 1997. Phototoxicity of individual polycyclic aromatic hydrocarbons and petroleum to marine invertebrate larvae and juveniles. Environ. Toxicol. Chem. 16, 2190–2199. https://doi.org/10.1002/etc.5620161029.

Pires, A.M., Branco, J.A., Picado, A., Mendonça, E., 2002. Models for the estimation of a 'no effect concentration'. Environmetrics 13, 15–27. https://doi.org/10.1002/env.501.

R Core Team, 2020. R: A Language and Evironment for Statistical Computing. Ver. 4.0.2. R Foundation for Statistical Computing, Vienna, Austria https://www.R-project.org/. (Accessed 5 June 2020).

Randall, C.J., Negri, A.P., Quigley, K.M., Foster, T., Ricardo, G.F., Webster, N.S., et al., 2020. Sexual production of corals for reef restoration in the Anthropocene. Mar. Ecol. Prog. Ser. 635, 203–232. https://doi.org/10.3354/meps13206.

Redman, A.D., Parkerton, T.F., 2015. Guidance for improving comparability and relevance of oil toxicity tests. Mar. Pollut. Bull. 98, 156–170. https://doi.org/10.1016/j.marpolbul.2015.06.053.

Redman, A.D., Parkerton, T.F., McGrath, J.A., Di Toro, D.M., 2012. PETROTOX: an aquatic toxicity model for petroleum substances. Environ. Toxicol. Chem. 31, 2498–2506. https://doi.org/10.1002/etc.1982.

Redman, A.D., Parkerton, T.F., Leon Paumen, M., Butler, J.D., Letinski, D.J., den Haan, K., 2017. A re-evaluation of PETROTOX for predicting acute and chronic toxicity of petroleum substances. Environ. Toxicol. Chem. 36, 2245–2252. https://doi.org/10.1002/etc.3744.

Renegar, D.A., Turner, N.R., 2021. Species sensitivity assessment of five Atlantic scleractinian coral species to 1-methylnaphthalene. Sci. Rep. 11, 529. https://doi.org/10.1038/s41598-020-80055-0.

Renegar, D.A., Turner, N.R., Riegl, B.M., Dodge, R.E., Knap, A.H., Schuler, P.A., 2017. Acute and subacute toxicity of the polycyclic aromatic hydrocarbon 1-methylnaphthalene to the shallow-water coral *Porites divaricata*: application of a novel exposure protocol. Environ. Toxicol. Chem. 36, 212–219. https://doi.org/10.1002/etc.3530.

Ricardo, G.F., Jones, R.J., Clode, P.L., Humanes, A., Negri, A.P., 2015. Suspended sediments limit coral sperm availability. Sci. Rep. 5, 18084. https://doi.org/10.1038/srep18084.

Ricardo, G.F., Jones, R.J., Clode, P.L., Humanes, A., Giofre, N., Negri, A.P., 2018. Sediment characteristics influence the fertilisation success of the corals *Acropora tenuis* and *Acropora millepora*. Mar. Pollut. Bull. 135, 941–953. https://doi.org/10.1016/j.marpolbul.2018.08.001.

Rinkevich, B., Loya, Y., 1979. Laboratory experiments on the effects of crude oil on the Red Sea coral *Stylophora pistillata*. Mar. Pollut. Bull. 10, 328–330. https://doi.org/10.1016/0025-326X(79)90402-8.

RStudio Team, 2020. RStudio: Integrated Development for R. RStudio, PBC, Boston, MA http://www.rstudio.com/. (Accessed 26 August 2020).

Schmidt-Roach, S., Miller, K.J., Woolsey, E., Gerlach, G., Baird, A.H., 2012. Broadcast spawning by *Pocillopora* species on the Great Barrier Reef. PLoS One 7, e50847. https://doi.org/10.1371/journal.pone.0050847.

Shlesinger, T., Loya, Y., 2019. Breakdown in spawning synchrony: a silent threat to coral persistence. Science 365, 1002. https://doi.org/10.1126/science.aax0110.

Singer, M.M., Aurand, D., Bragin, G.E., Clark, J.R., Coelho, G.M., Sowby, M.L., et al., 2000. Standardization of the preparation and quantitation of water-accommodated fractions of petroleum for toxicity testing. Mar. Pollut. Bull. 40, 1007–1016. https://doi.org/10.1016/S0025-326X(00)00045-X.

Sorokin, I.I., 2013. Coral reef ecology. Vol. 102 of Ecological Studies. Springer Science & Business Media, New York; Berlin, p. 465.

Storrie, J., 2011. Montara wellhead platform oil spill - a remote area aesponse. International Oil Spill Conference Proceedings. vol. 2011 pp. Abstract 159.

Sun, S., Lu, Y., Liu, Y., Wang, M., Hu, C., 2018. Tracking an oil tanker collision and spilled oils in the East China Sea using multisensor day and night satellite imagery. Geophys. Res. Lett. Vol. 0. https://doi.org/10.1002/2018GL077433.

Suzuki, G., 2012. Simultaneous spawning of *Pocillopora* and *Goniopora* corals in the morning time. Galaxea J. Coral Reef Stud. 14, 115–116. https://doi.org/10.3755/galaxea.14.115.

The Guardian, 2018. Emergency declared after oil spill ignites on Indonesian island of Borneo. https://www.theguardian.com/world/2018/apr/04/emergency-declared-after-oil-spill-ignites-on-indonesian-island-of-borneo. (Accessed 21 April 2018).

Turner, N.R., Renegar, D.A., 2017. Petroleum hydrocarbon toxicity to corals: a review. Mar. Pollut. Bull. 119, 1–16. https://doi.org/10.1016/j.marpolbul.2017.04.050.

USEPA UEPA, 2012. Estimation Programs Interface SuiteTM for Microsoft1 Windows, Ver 4.11 (Washington, DC).

Villanueva, R., Montaño, M., Yap, H., 2008. Effects of natural gas condensate-water accommodated fraction on coral larvae. Mar. Pollut. Bull. 56, 1422–1428. https://doi.org/10.1016/j.marpolbul.2008.05.008.

Warne, M., Batley, G., van Dam, R., Chapman, J., Fox, D., Hickey, C., et al., 2018. Revised Method for Deriving Australian and New Zealand Water Quality Guideline Values for Toxicants. Prepared for the Revision of the Australian and New Zealand Guidelines for Fresh and Marine Water Quality. Australian and New Zealand Governments and Australian State and Territory Governments, Canberra, Australia.

Willis, B.L., Babcock, R.C., Harrison, P.L., Wallace, C.C., 1997. Experimental hybridization and breeding incompatibilities within the mating systems of mass spawning reef corals. Coral Reefs 16, S53–S65. https://doi.org/10.1007/s003380050242.

Woo, S., Lee, A., Denis, V., Chen, C., Yum, S., 2013. Transcript response of soft coral (*Scleronephthya gracillimum*) on exposure to polycyclic aromatic hydrocarbons. Environ. Sci. Pollut. Res. 21, 901–910. https://doi.org/10.1007/s11356-013-1958-5.

Xiang, N., Jiang, C., Huang, W., Nordhaus, I., Zhou, H., Drews, M., et al., 2019. The impact of acute benzo(a)pyrene on antioxidant enzyme and stress-related genes in tropical stony corals (*Acropora* spp.). Sci. Total Environ. 694, 133474. https://doi.org/10.1016/j.scitotenv.2019.07.280.